4

CHIRAL POLYESTERS CONTAINING AZOMESOGENS FOR NONLINEAR OPTICS: ROLE OF STEREOCHEMISTRY OF CHIRAL MOLECULES

4.1. Introduction

Chiral materials can provide new approaches to second-order nonlinear optics. Chiral molecules possess no reflection symmetry and occur in two enantiomers that are mirror images of each other. Such molecules are essentially noncentrosymmetric with a nonvanishing electric-dipole allowed second-order response. Early research into second-order nonlinear optical materials for applications in frequency conversion and linear electro-optic modulation and conversion has focused mainly on polar molecules due to the requirement for non-centrosymmetric media.[1-3] Even in the absence of strong interaction between donor-acceptor groups, chiral medium is showing nonlinear response and persist even in macroscopic samples with high symmetry.[4,5] In such macroscopic dimensional chiral structures, the poling of chromophores can be achieved through chemical synthesis, and there is no need for external poling.[6-8] While nonlinear optical processes at chiral surfaces and in homopolymeric polar, chiral media have received considerable attention,[9-13] here, the use of chirality in copolymeric polar bulk media for exploiting practical materials has been considered seriously. This chapter has focused on both molecular and supramolecular aspects.[14-16] The molecular aspects that couple to the macroscopic response depend both on the details of the molecular structure and on the macroscopic symmetry group to which the molecule belongs. It is found that stereochemistry of polar chiral molecules plays a vital role in exploiting large second order nonlinear optical responses.

Azomesogen (azobenzene) polymers are receiving considerable attention because of their potential use in various photonic applications.[17-19] These azomesogen polymers are usually NLO chromophore-functionalized polymer systems which are superior to the guest-host NLO polymer systems in many aspects such as stability,

homogeneity, processing etc. In dye-functionalized polymers, the dye molecules are covalently bonded to the polymer backbone; hence, two chemical entities, which are joined together on a molecular level, offer greater stability than the guest-host polymer system. The NLO dye molecules can be covalently attached to the linear chain of a polymer by simple chemical processes.[2]

This chapter discusses the development of polyesters having main chain chirality and at the same time with push-pull (donor-acceptor) azobenzene moiety. Due to the prevailing chirality of the main chain and the directional orientation (preferably *trans*) of the azobenzene group, the polyesters are organized with a Λ helical conformation in space. Polymers with such organized geometry are very interesting since they can supplement the directional order of donor-acceptor π electron system and the dipole units are tilted in one direction along the polymer axis which leads to high second harmonic generation efficiency.[7, 20] This approach helps to satisfy both the essential and necessary conditions for a material to be NLO active (Second harmonic generation); achieving both spatial asymmetry and charge asymmetry with out poling. Main chain chirality induces chemical poling. This results in the enhancement of SHG efficiency of the polyesters. Synthetic polymers, which are so far used for NLO applications, are poled with corona discharge at temperatures around their glass transition temperature. During poling, many polymers undergo darkening (loss of optical transparency) and once the external field is removed, they undergo relaxation to the unoriented state, there by losing the NLO activity. In the present case, since poling is not used, such problems are avoided. The synthesis of chiral main-chain NLO polyesters were carried out by a facile way which involved the polycondensation of chiral units and donor-acceptor π-conjugated azomesogen chromophores.[14-16] The work on this subject, focuses on molecular and supramolecular aspects of material design based on molecular stereochemistry. The approach to this problem parallels that which has been so successful in optimizing copolymeric systems. First consideration was the stereochemistry of the chiral molecules. Along with that the molecular features that might contribute to hyperpolarizability were examined. The focus was on polymer design, synthesis, and characterization. Finally, the supramolecular arrangements of

optimized copolymeric structures that best exploit the molecular response were synthesized. The systematic analysis of the relevant molecular quantities and the experimental measurement described here will result in technologically interesting chiral nonlinear optical materials.

4.2. Computational methods

4.2.1. Monomers

The monomers considered in this study are shown in **Figure 4.1** and **Figure 4.4**. All the monomers, diastereomers of chiral molecules and azomesogen chromophores, have been optimized using restricted B3LYP formalism in density functional theory (DFT) using 6-31+G(d,p) basis set available in the Gaussian algorithm.[21-25] Since DFT methods give more accurate results (with electron correlation) than semiempirical calculations, which are done at extremely minimal (Slater type orbitals) basis set; (electron correlation is only included implicitly by the parameters), and less computationally demanding for geometry optimization compared to *ab initio* methods (with high electron correlation), all the geometry optimizations of monomers have been done by DFT methods. The optimized geometries were used to compute the SCF MO energies. The *static* spectroscopic properties of monomers have been calculated using Coupled Perturbed Hartree-Fock (CPHF) method at RHF 6-31++G(d,p) level available in the Gaussian codes.[26] The *dynamic* spectroscopic properties have been calculated using the Zerner's INDO SOS method with sum over 82 states.[27] Theoretical value of optical rotation have been calculated using frequency dependent, *ab initio,* Hartree-Fock /6-31G(d) level of theory at a wavelength of 500 nm using Gaussian algorithm.[28,29]

4.2.2. Polymers

All the polymer geometries (repeating units) were optimized using the AM1 parameterized Hamiltonian available in the Gaussian 03 set of codes.[30] The geometries obtained by AM1 calculations have been compared with geometries obtained using DFT based methods at B3LYP/6-31+(d,p) level for one of the polymers. Both the geometries have comparable bond lengths and bond angles. Compared to the small changes in bond length and bond angle, the computational demand for DFT method is much more for

polymers. Hence, geometry calculations are restricted to semiempirical level. The optimized geometries were used to compute the SCF MO energies. Because of the very high cost of computation in calculating the properties of polymers (repeating units) using polarized and diffused basis sets, *static* molecular properties of polymers have been limited to 6-31G(d) basis set level[26] The *dynamic* spectroscopic properties have been calculated using the Zerner's INDO-SOS method with sum over 82 states.[27]

4.3. Designing of molecules

While designing the chiral monomers, the main consideration was about the stereochemistry of the chiral molecules. Stereochemistry is the study of the spatial arrangements of atoms in molecules and complexes. Stereoisomers (stereomers) are molecules with the same atoms and bond structure, but different three-dimensional arrangements of atoms. Stereoisomers can be divided into two categories of enantiomers (mirror images) and diastereomers (non-mirror images). Here 4 pairs of diastereomers are selected for the stereochemical study. The other chromophores were selected on the basis of push-pull donor-acceptor systems and the ability to form polycondensation polymers with the chiral monomers. Design of polymers, which are incorporated with the previously designed monomers, was based on chirality and push pull donor acceptor strength of the whole system, so as to obtain systems with more pronounced NLO activity (higher value of β).

4.3.1. Monomer design

4.3.1.1 Chiral molecules

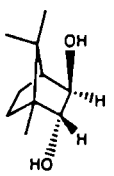

(1R, 2*R*, 3*R*, 4*S*)-Camphanediol

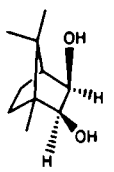

(1R, 2*S*, 3*R*. 4*S*)-Camphanediol

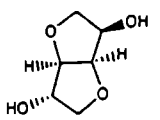

Isosorbide

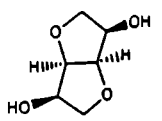

Isomanide

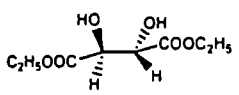

(2*R*,3*R*)-diethyl tartrate

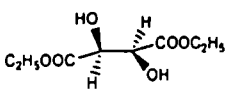

(2*R*,3*S*)-diethyl tartrate

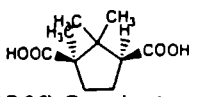

(1*R*,3*S*)-Camphoric acid

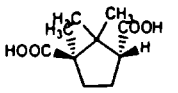

(1*R*,3*R*)-Camphoric acid

Figure 4.1. Chiral monomers

Four pairs of diastereomers have been selected as chiral monomers. All are dipolar chiral molecules. They are shown in **Figure 4.1.** In these diastereomers (1R, 2R, 3R, 4S) camphanediol [(exo-endo) camphanediol)] and (1R, 2S, 3R, 4S) camphanediol [(exo-exo) camphanediol)] are bicyclic bridged chiral molecules, 1,4:3,6-Dianhydro-D-sorbitol (isosorbide) and 1,4:3,6-Dianhydro-D-mannitol (isomanide) are bicyclic and heterocyclic chiral molecules. (2R, 3S) diethyl tartrate (*meso*) and (2R, 3R) diethyl tartrate are linear chiral molecules and (1R,3R) camphoric acid (exo-endo) and (1R, 3S) camphoric acid [(D(+) or (exo -exo)] are moncyclic chiral molecules.

4.3.1.1.1. Static and dynamic molecular property calculations

4.3.1.1.1.a. Dipole moment

The values of static and dynamic dipole moments are given in **Table 4.1.**

Table 4.1: Dipole moment of monomers in units of debye

Diastereomers	μ_x	μ_Y	μ_Z	μ_g *Static*	μ_g *Dynamic*
Camphanediol (exo-endo)(I)	1.5521	-0.6410	-0.7251	1.8291	11.2647
Camphanediol (exo-exo)(II)	-1.2250	2.1911	-2.2158	3.3483	12.5664
Isosorbide(III)	-0.3463	1.6845	1.8690	2.5398	15.6456
Isomanide(IV)	-0.6458	1.8237	-0.6505	2.0410	11.7278
(2R,3S)Diethyl tartrate(V)	0	0	0	0	0
(2R,3R) Diethyl tartrate(VI)	-3.3116	-1.1773	-0.2488	3.5234	19.3087
Camphoric acid (exo-endo)(VII)	0.9096	2.2003	0.5283	2.4388	20.0525
Camphoric acid (exo-exo)(VIII)	0.4233	0.6856	1.8312	2.0007	16.6195

From the **Table 4.1** it is clear that one of the diastereomers in each pair has higher dipole moment than the other. This is due to the orientation of the dipolar group. The selection of diastereomers was based on this dipolar orientation. In one of the diastereomers, the dipoles are oriented to the same direction (eg. exo-exo), while in the other isomer the orientation is through opposite directions (eg. exo-endo). The

expectation was that the diastereomers with oppositely oriented dipoles have smaller value of dipole moment. But while analyzing the geometries, after optimization, it could be found that the ground state dipole moment,μ_g of isosorbide (oppositely oriented dipoles) is greater than that of isomanide. In camphoric acid pair, the same has been observed; exo-exo isomer has the higher value than exo-endo pair. This is because in isosorbide, isomanide and camphoric acid diastereomers, the optimized output geometry is more stable (twist and chair forms respectively), than the planar input geometry. In the optimized geometries of camphanediol and diethyl tartrate, diastereomers are not changed much. The blue arrow in **Figure 4.2.** shows the direction of net dipole moment in isosorbide and isomanide. In this twist conformation of isosorbide, the arrangement of oppositely oriented dipoles are in favor of the dipole moment through resultant direction, while in the twist conformation of isomanide, the orientation of dipoles is not in favor of the direction of resultant dipole moment vector (**Figure 4.2.**). In the optimized chair conformation of camphoric acid (exo-exo), the same has been true, the orientations of dipoles are not favoring the resultant dipole moment vector. Hence, a decrease in the value of dipole moment for the (exo-exo) isomer of camphoric acid. In the other two pairs, the optimized geometry has not been changed much from the planar input geometry. Thus, for those pairs of diastereomers, the resultant dipole moments are as expected from the input geometry.

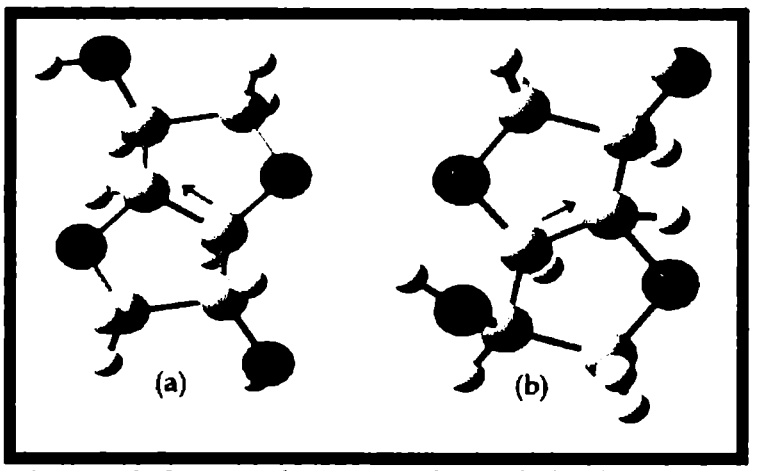

Figure 4.2 .Optimized sturcture of Isosorbide (a) and Isomanide(b)

4.3.1.1.1.b. Polarizability (α)

Table 4.2 gives the polarizability values. For all pairs of diastereomers, the polarizability is almost equal. Thus, it can be concluded that polarizability does not depend much on the dipolar orientation.

Table 4.2: Polarizability α of diastereomers

Diastereomers	α_{xx}	α_{yy}	α_{zz}	*α (au)*	α_{tot} * *(esu)$ x10^{-23}*	α_{tot}** *(esu)$ x10^{-23}*
Camphanediol (exo-endo)	107.2152	112.8685	109.4957	109.8598	1.6279	38.9
Camphanediol (exo-exo)	109.7963	110.0699	109.9183	109.9282	1.6289	38.9
Isosorbide	87.1126	66.6235	71.0871	74.9411	1.1105	38.3
Isomanide	84.8408	68.1332	70.6659	74.5466	1.1046	37.3
(2R,3S)Diethyl tartrate	127.7344	107.5076	85.3803	106.8741	1.5837	97.4
(2R,3R) Diethyl tartrate	98.2089	106.3238	114.7136	106.4155	1.5769	83.3
Camphoricacid(exo-endo)	118.3098	108.8939	114.6224	113.9420	1.6884	94.0
Camphoric acid(exo-exo)	121.6146	107.3292	113.8367	114.2602	1.6931	102.0

*$\alpha (esu) = 0.148185x10^{-24}$ α (au) *Static values, ** Dynamic values*

4.3.1.1.1.c. Hyperpolarizability (β)

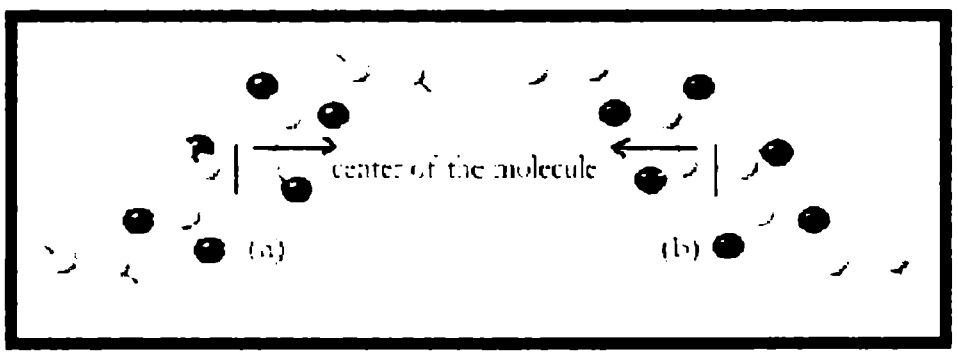

Figure 4.3. Diastereomers of diethyl tartrate, (2R, 3R) (a) and (2R,3S) (b)

Ab initio calculations using Hartree-Fock CPHF level is used to predict the second order NLO response. From the results of *static* CPHF calculations in **Table 4.3**, it can be observed that, in spite of the similar values of α obtained for the diastereomers,

the β values have been found to vary considerably according to the stereochemistry of the diastereomer. For (2R, 3S) Diethyl tartrate β value is zero while (2R, 3R) diethyl tartrate has comparatively good β value. This is because of the presence of reflection center (center of symmetry) in the former (**Figure 4.3**) In the case of isomanide and isosorbide, β value is almost doubled in isomanide compared to isosorbide. The variation in β value with respect to the stereochemistry of camphanediol and camphoric acid diastereomers are not highly pronounced. But in perspective of designing the chiral molecule with good β values, (2S, 3R) -camphanediol (exo-exo) can be selected as a promising candidate.

Table 4.3: HOMO-LUMO Gap (ΔE) in eV, Ground-State Dipole Moment (μ_g) in debye, Linear Polarizability (α) in units of 10^{-23} esu, and First Hyperpolarizability (β) in units of 10^{-30} esu for the diastereomers (ab initio CPHF static property calculations)

Diastereomers	ΔE	μ_g	α	β_{vec}
Camphanediol (exo-endo)	0.4392	1.8291	1.6280	1.0793
Camphanediol (exo-exo)	0.4334	3.3484	1.6290	1.2765
Isosorbide	0.4572	2.5398	1.1105	0.3370
Isomanide	0.4625	2.0411	1.1047	0.6936
(2R,3S)Diethyl tartrate	0.4803	0	1.5837	0
(2R,3R) Diethyl tartrate	0.4741	3.5234	1.5769	0.4938
Camphoric acid (exo-endo)	0.4729	2.4388	1.6885	0.3102
Camphoric acid (exo-exo)	0.4703	2.0007	1.6932	0.3527

According to donor-acceptor concept, the major contribution to β is due to charge transfer. Thus, one will get higher β with the factors that enhance the charge transfer. The HOMO-LUMO gap in the molecular orbital picture plays a vital role in the charge transfer.[30] If the gap is small, it is very easy for the charge transfer to occur. Thus the HOMO largely dictates the source of charge transfer and the details of the molecular LUMO govern the acceptor portion of the excitation. One can tailor the asymmetry of the electron density by tuning the energetics (HF-SCF) of the molecule. The HOMO-LUMO gap (ΔE) of the molecules are given in **Tables 4.3.** There is not much difference in

the HOMO-LUMO gap of each pairs of diastereomers with respect to their stereochemistry. Also, while examining the values of β with respect to corresponding μ values of the respective diastereomer, especially for isosorbide-isomanide pair and camphoric acid pair, it can be seen that the HOMO-LUMO, charge transfer model is inadequate for explaining the difference in β value of chiral molecules in the perspective of stereochemistry.

Dynamic (frequency dependent) Sum Over States (SOS) calculations will give a more transparent idea about the relationship between the first hyperpolarizability and stereochemistry of different diastereomers. Since CPHF method is a frequency independent model, only static fields are considered. But in the SOS method frequency equal to that of Nd:YAG laser (1024 nm,1.67 eV) has been applied as the field.

Table 4.4: Oscillator strength (f), Optical Gap (δE) in eV, Ground-State Dipole Moment (μ_g) in debye, Difference in dipole moment between ground state and excited state (Δμ), Linear Polarizability (α) in units of 10^{-23} esu, and First Hyperpolarizability (β) in units of 10^{-30} esu for the diastereomers (ZINDO-SOS dynamic property calculations)

Diastereomers	*f*	δE	Δμ	μ_g	α	β_{vec}
Camphanediol (exoendo)	0.0173	13.5077	15.2618	11.2648	38.9	1.5634
Camphanediol (exoexo)	0.0292	13.3466	32.7791	12.5664	38.9	2.0995
Isosorbide	0.0343	10.9403	11.1665	15.6456	38.3	0.3135
Isomanide	0.0360	11.0660	23.7540	11.7278	37.3	3.2238
(2R,3S) Diethyltartrate	1.0042	8.7724	0	0	97.4	0
(2R,3R) Diethyltartrate	0.5121	8.6951	5.7691	19.3088	83.3	6.7476
Camphoricacid (exo,endo)	0.4561	8.9083	1.2877	20.0526	94.0	1.4652
Camphoricacid (exo-exo)	0.6857	8.8184	6.7321	16.6195	100.2	5.7858

Table 4.4. reports the two-level parameters such as, magnitude of oscillator strength (*f*), the optical gap (δE), the difference between the dipole moments of ground-state and the excited state (Δμ), the ground-state dipole moment (μ_g), the linear polarizability (α), and the first hyperpolarizability (β) of the *dynamic* SOS calculation.

Even in the presence of applied field (1.67ev = 1024nm, Nd:YAG frequency), the trend is same as that of *static* calculation. In the case of isosorbide and isomanide, the difference in β value is more prominent, in one order of magnitude. As a chiral molecule exo-exo-camphanediol has shown good second order response while applying the frequency dependent experimental conditions also. It can be seen that exo-exo-camphoric acid is the best among them under the experimental conditions. Consider the first pair, camphanediol diastereomers. Oscillator strength is low and optical gap is higher for exo-endo diastereomer. Both the factors decrease the β value of exo-endo isomer. Also, the $\Delta\mu$ value is higher in exo-exo isomer (almost doubled). Thus in camphanediol pair, the exo-exo isomer has a higher value of β. In diethyl tartrate pair, for the (2R, 3S) diastereomer the β value is zero, i.e. (2R, 3S) diethyl tartrate is not active towards second order NLO properties. This is because of the center of symmetry present in the molecule (center of inversion). The ground state dipole moment and the change in dipole moment are also zero because of this center of inversion. But it has a comparatively high α value compared to all other isomers. Since there is no inversion center in (2R, 3R) diethyl tartrate, and has comparatively large change in dipole moment and oscillator strength, it has got the highest β value. Hence, it can be taken as a potential chiral molecule for second order NLO applications.

While examining the isosorbide-isomanide pair and camphoric acid pair, it can be seen that the β values vary drastically with respect to the stereochemistry of the diastereomer. In isomanide, it is increased in one order of magnitude. Even though the ground state dipole moment μ, is large for isosorbide, and exo-endo camphoric acid, the change in dipole moment $\Delta\mu$, is higher for isomanide and exo-exo camphoric acid, which mainly determines the value of β. In fact, the optical gap for isomanide is slightly larger than that of isosorbide, but the large difference in $\Delta\mu$ governs β.

To get a clear picture about the dependence of stereochemistry on the β value, all the determining parameters of β, *(f, δE Δμ)*, have been observed thoroughly. It can be seen that for the diastereomer with large $\Delta\mu$ value, the β is also large. According to

Lalama *et al* [31] the dipole moment difference Δμ, between the ground and excited state is the major contributing factor in determining the value of β vector. Also it is stated that, if in Δμ , any of the components are absent (eg, y or z component), the contribution to β vector from those directions is also negligible and the major contribution of β is obtained from the charge transfer direction.

Table 4.5: Dipole moment difference between the ground state and excited state in units of debye

Diasteromer	$\Delta\mu_x$	$\Delta\mu_y$	$\Delta\mu_z$	$\Delta\mu$	β_{vec}
Camphanediol (exo-endo)	-0.5175	-12.8195	-8.2654	15.2618	1.5634
Camphanediol (exo-exo)	22.7667	-22.6128	-6.6937	32.7791	2.0995
Isosorbide	-3.9535	-1.5985	12.1870	12.9115	0.3135
Isomanide	22.4625	6.9725	3.3271	23.7540	3.2238
(2R,3S)Diethyl tartrate	0	0	0	0	0
(2R,3R) Diethyl tartrate	-5.3848	-0.5686	-1.9909	5.7691	6.7476
Camphoric acid (exo-endo)	-0.5645	0.7021	-0.9201	1.2877	1.4652
Camphoric acid (exo-exo)	6.5060	0.8467	1.5086	6.7321	5.7858

The value of components of Δμ are summarized in **Table 4.5.** It is very clear that the major contribution of the Δμ is coming from the *z* direction and it is the direction of charge transfer in all the optimized geometries. Also, it is well pronounced that the Δμ and $\Delta\mu_x$ values are also higher in the diastereomers with higher value of β. Thus the β has a strong dependence on stereochemistry of the chiral molecule through the dipole moment difference between the ground state and the excited state, Δμ and the direction of its major component (μ_x, μ_y, μz). Thus, in designing the chiral molecules the stereochemistry is very important.

4.3.1.1.1.d. Chiral component

Since microscopic first hyperpolarizability, β is a 3rd rank tensor, it has 27 tensor components. But in the general case of a molecule with no symmetry, these 27 elements are reduced to 10 according to Kleinman symmetry for second harmonic generation β (2ω; ω, ω). Due to independent interchange of Cartesian coordinates, $\beta_{ijk} = \beta_{ikj}$. These

irreducible 10 tensor components are β_{xxx}, β_{xxy}, β_{xyy}, β_{yyy}, β_{xxz}, β_{xyz}, β_{yyz}, β_{xzz}, β_{yzz}, and β_{zzz}.[1,32-35] By taking the tensor product of these 10 tensor components, orientationally averaged hyperpolarizabilities can be calculated from the equations given below.[36]

$$\beta_{vec}(-2\omega;\omega,\omega) = \sqrt{\beta_X^2 + \beta_Y^2 + \beta_Z^2} \qquad 4.1$$

where

$$\beta_i = \sum_{j=x,y,z} \frac{\beta_{ijj} + \beta_{jij} + \beta_{jji}}{3} \quad ; \quad i = x, y, z \qquad 4.2$$

In an electric dipole approximation, the tensor component β_{xyz} is the chiral component of the medium and all other nine tensor components are achiral. Because of the property of symmetric tensor product basis set elements, the value of β_{xyz} has become zero in the tensor product. But the chiral component β_{xyz} becomes non-zero and contribute a major portion to the macroscopic (3-D) second order polarizability tensor, χ_{XYZ}.[8, 11,12, 37,38] Thus while designing the chiral molecule with high β value, the β_{xyz} component becomes important in macroscopic perception. The molecule with large chiral (β_{xyz}) component should give high value for macroscopic second harmonic generation. The molecules which are more symmetric (less chiral) will have small values of the chiral component β_{xyz}.

From **Table 4.6,** it is very clear that chiral component β_{xyz} is substantially higher for most of the chiral molecules. Also, it is very much dependent on the stereochemistry of the chiral molecule. Exo-exo camphanediol, isomanide, (2R, 3R) diethyl tartrate, exo-exo camphoric acid is the potential chiral candidate in each pair with respect to the chiral component β_{xyz} and stereochemistry. And hence, these four diastereomers will give a major chiral contribution to the macroscopic SHG, χ_{XYZ}. Thus, these are used as promising chiral molecules for constructing chiral media or incorporating in to a polymer chain to get a chiral medium with pronounced SHG

As a crude approximation, the stereochemistry and chirality can be related to each other through the optical rotation $[\alpha]_D$. Optical rotation is a property, by virtue of which the polarized light rotates its plane. Chirality is the necessary and sufficient

condition for optical rotation and the stereochemistry of the molecule determines the amount and the direction of rotation. From **Table 4.6,** it is clear that, the value of chiral component always agrees with the optical rotation of the diastereomer. The specific rotation of diastereomeric pair, isomanide and isosorbide are available in literature. It is $+45^0$ for isosorbide and $+89^0$ for isomanide. So there is not much surprise in the large value of chiral component obtained for isomanide compared to isosorbide. Circular dichorism will give a vivid picture about the chirality and chirality parameter, which is beyond the scope of this work due to the non-availability of the CD spectrometer. It can be concluded that, the stereochemistry of the small molecule and the conformation of its macroscopic forms are very important in determining the chiral component and thus macroscopic SHG.

Table 4.6: ***First hyperpolarizabilities of diastereomers β (Static) in units of au***

β *Tensors*	*Camphane diol (exo-endo)*	*Camphane-diol (exo-exo)*	*Iso sorbide*	*Iso manide*	*Diethyl-tartrate (2R,3S)*	*Diethyl-tartrate (2R,3R)*	*Camphoric-acid (exo-endo)*	*Camphoric-acid (exo-exo)*
β_{xxx}	-3.5622	14.6356	-6.423	38.0264	0	39.2226	27.9278	43.9083
β_{xxy}	39.8690	28.6849	6.5766	-20.1099	0	6.8411	-3.8573	9.5022
β_{xyy}	-3.6198	1.3465	-6.4437	-0.2094	0	-11.2329	-21.5895	-32.9704
β_{yyy}	58.5435	38.0116	18.1242	-34.0895	0	4.7007	21.7921	-26.1922
β_{xxz}	11.4376	-15.7655	6.5635	18.9935	0	-25.6202	6.4420	23.4927
β_{xyz}	-1.890	-5.7218	-1.3220	-7.4538	0	1.5503	15.7178	-19.9288
β_{yyz}	-6.7104	-43.1634	2.5726	-4.7536	0	-12.0035	20.1586	-5.2109
β_{xzz}	7.4152	0.0678	2.7583	2.1477	0	18.8723	-13.5133	-23.3222
β_{yzz}	26.2109	8.6866	0.1008	-7.1146	0	13.7831	-9.1267	-20.0598
β_{zzz}	4.0111	-67.1371	19.2154	18.7612	0	16.8920	7.4571	-5.5366
β_X	0.2332	16.0500	-10.108	39.9647	0	46.8620	-7.1751	-12.3844
β_Y	124.6233	75.3831	24.8016	-61.314	0	25.3249	8.8082	-36.7498
β_Z	8.7384	-126.066	28.3516	33.0011	0	-20.7317	34.0577	12.7453
β_{vec}*	124.9295	147.7594	39.0015	80.2849	0	57.1594	35.9025	40.8211
β_{vec}**	1.0793	1.2765	0.3369	0.6936	0	0.4938	0.3102	0.3525
$[\alpha]_D$#	-35.70	-42.48	+49.31	+80.69	0	+150.97	+46.47	+29.27

* β_{vec} *in atomic units,* ** β_{vec} *x* 10^{-30} *in esu,* β *(*10^{-32} *esu) = 0.863916*β *(au), # calculated specific rotation*

4.3.1.2. Azomesogen chromophores

The azomesogen chromophores have been designed on the basis of donor-acceptor capacity and the ability to form polymers with the previously designed chiral molecules by easy polycondensation method. They are, bis(4-hydroxyphenylazo)-2,2'-dinitrodiphenylmethane (BHDM) and azobenzene-4,4'-dicarbonyl chloride (AZCl) (**Figure 4.4.**) The former is Λ shaped chromophore with donor-acceptor push-pull groups. The later is a diacid chloride; the most suitable reactant for an -OH group condensation. The results are given in **Table 4.7**

Table 4.7: ***Static values of HOMO-LUMO gap (ΔE), dipole moment μ, in debye polarizability (α) in units of α 10^{-23} esu, Chiral component of Hyperpolarizability β_{xyz} in au, total Hyperpolarizability (β_{vec})* in au and β_{vec} ** in 10^{-30} esu***

Chromophore	*ΔE*	μ	α	β_{xyz}	β_{vec}*	β_{vec} **
BHDM	0.3228	2.5498	5.5642	8.7870	935.9275	8.0856
AZCl	0.3308	3.4606	3.4307	-0.0641	116.584	1.0071

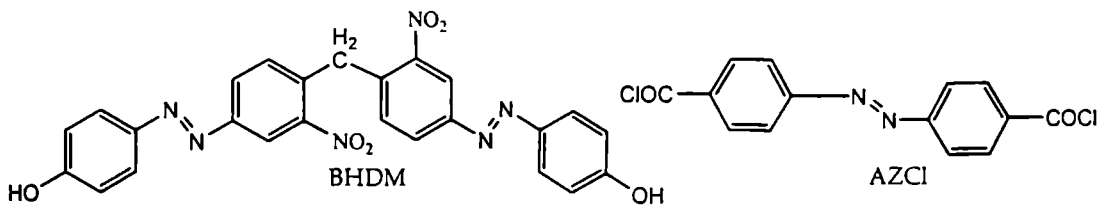

Figure 4.4. Azomesogen chromophores

It is clear that both the molecules, bis(4-hydroxyphenylazo)-2,2'-dinitrodiphenylmethane (BHDM) and azobenzene-4,4'-dicarbonyl chloride (AZCl) are very good NLO active chromophores with high microscopic SHG values. But the value of chiral component is almost negligible in AZCl compared to the total β value (0.075%). The β_{xyz} in BHDM (0.9%) is also negligible compared with the very high β_{xyz} of exo-exo

camphanediol (50%). But the HOMO-LUMO gap is small in these chromophores compared to the chiral molecules. This will help easy charge transfer. When these chromophores form polymers with the early designed chiral molecules, the macroscopic structures should be more chiral than the homopolymer of these chromophores. Hence, these resultant polymers should have high value of β due to the charge transfer and also due to chirality.

From the *Dynamic SOS* calculation also, (**Table 4.8**) it can be observed that the chromophores have very good beta value with high oscillator strength and low optical gap compared to the chiral molecules and which will form very good NLO active polymers with the chiral molecules.

Table 4.8: Oscillator strength (f), Optical Gap (δE) in eV, Ground-State Dipole Moment (μ_g) in debye, Difference in dipole moments between ground state and excited state (Δμ), Linear Polarizability (α) in units of 10^{-23} esu, and First Hyperpolarizability (β), in units of 10^{-30} esu for the chromophores (ZINDO-SOS dynamic property calculations)

Chromophore	*f*	δE	Δμ	μ_g	α	β
BHDM	5.3825	3.6829	19.6174	110.7927	1100	488.9864
AZCl	1.3355	4.1932	3.365	10.6268	927	106.8586

4.3.2 Polymer design

Polymers are designed as the condensation products of chromophores, bis(4-hydroxyphenylazo)-2,2′-dinitrodiphenylmethane (BHDM) and azobenzene-4,4′-dicarbonyl chloride (AZCl) with the previously designed chiral molecules. One repeating unit of each polymer has been considered for the optimization and molecular property calculations. Each repeating unit contains one molecule of bis(4-hydroxyphenylazo)-2,2′-dinitrodiphenylmethane (BHDM), two molecules of azobenzene-4,4′-dicarbonyl chloride (AZCl) and one chiral molecule. SHG properties have been compared with respect to 2-methyl-4- nitroaniline (MNA) as reference. The chiral effect has been studied by designing a repeating unit with out the chiral component. The structures of the polymers are given in **Figure 4.5.**

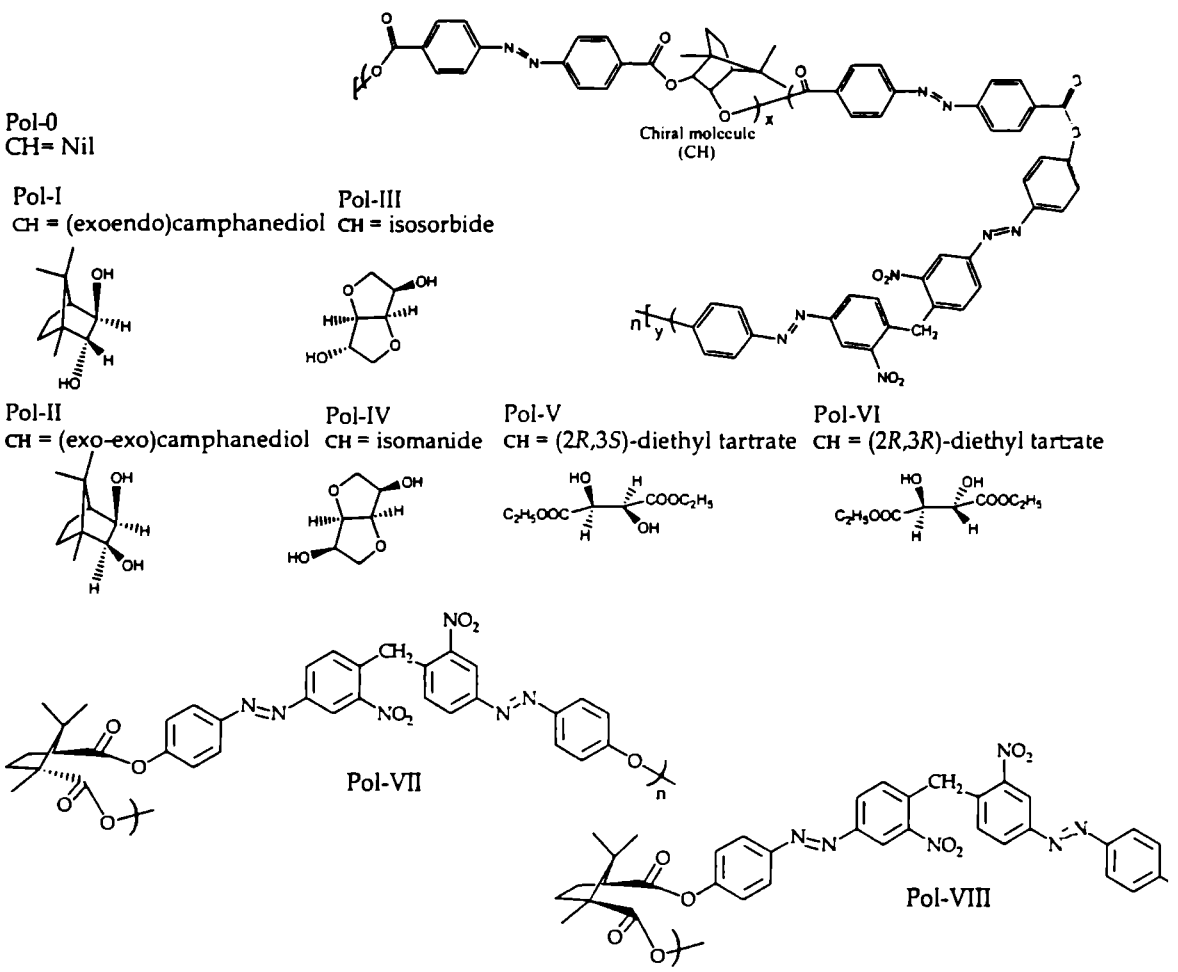

Figure 4.5. Structure of polymers

4.3.2.1 Static and dynamic molecular property calculations

4.3.2.1.a Dipole moment

The *static* and *dynamic* dipole moment values of polymers incorporating chiral molecules (**Pol-I** to **Pol-VIII**), the polymer without the chiral molecule (**Pol-0**) and that of 2-methyl-4-nitroaniline (MNA) are summarized in **Table 4.9.** It is clear that depending up on the stereochemistry of the chiral molecule; the corresponding polymer has shown variation in dipole moment. The resultant dipole moment of the polyesters is along the helical axis (**Figure 4.6**). The dipole moment orientation in polyesters matches with the early predicted dipole moment orientation of chiral monomer. (**Figure 4.7**). The dipole

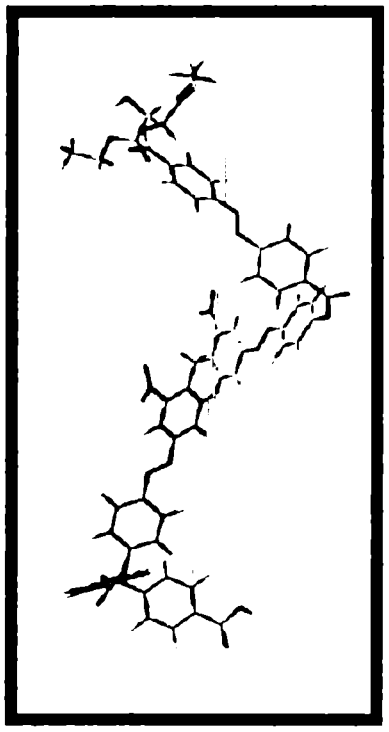

Figure 4. 6. Helical structure of polymer **Pol-V**. Green line indicates the direction of resultant dipole moment

moment values of MNA and the polymer without chiral molecule are close to that of polymers **Pol-I** to **Pol-VIII**.

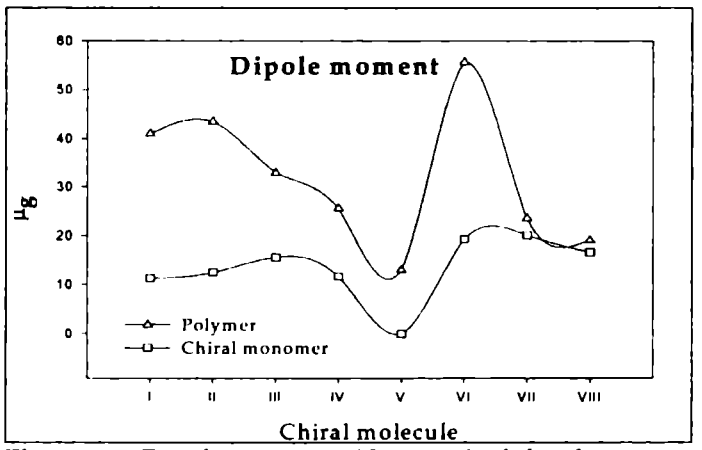

Figure 4.7: Dipole moments (dynamic) of chiral monomers and polymers (Repeating units) in units of debye

Table 4.9: Dipole moment of polymers in units of debye

Polymers	μ_x	μ_Y	μ_Z	μ_g *Static*	μ_g *Dynamic*
Pol-I	2.0609	0.0130	-5.0238	5.4301	41.0062
Pol-II	2.9365	-1.5043	-4.9535	5.9517	43.4733
Pol-III	5.5941	0.3901	-5.1517	7.6149	32.8368
Pol-IV	2.4274	0.4286	-2.8267	3.7505	25.6170
Pol-V	-2.6800	1.6986	1.6649	3.5832	13.1031
Pol-VI	1.8715	-3.5532	-4.0570	5.7085	55.6096
Pol-VII	-2.7721	4.2410	0.0377	5.0667	23.5744
Pol-VIII	-1.9494	4.0845	-0.2992	4.5357	19.0389
Pol-0	2.8049	0.4061	-2.1662	3.5672	33.1546
MNA	-5.9267	-1.3089	1.1946	6.1859	42.4044

4.3.2.1.b Polarizability (α)

In the case of polymers also, α values (**Table. 4.10.**) are not varying much with respect to the stereochemistry. But all the polymers have higher values than MNA.

Table 4.10:Polarizability α of polymers

Polymers	α_{xx}	α_{zz}	α *(au)*	α_{tot} *x10^{-23} Static**	α_{tot} *x10^{-23} Dynamic**
Pol-I	825.4632	590.4124	800.9117	11.8683	1170.0
Pol-II	825.2663	588.9055	800.9302	11.8686	1270.0
Pol-III	805.5283	546.0535	769.8875	11.4086	989.0
Pol-IV	790.4255	589.0701	764.6528	11.3310	960.0
Pol-V	815.2945	573.3554	795.8526	11.7934	1190.0
Pol-VI	803.6050	579.6060	477.1678	11.0709	1170.0
Pol-VII	329.2086	415.3341	468.7119	6.9456	1050.0
Pol-VIII	399.3801	415.9719	467.5593	6.9286	1040.0
Pol-0	716.7615	487.7200	702.6447	10.4122	950.0
MNA	118.5149	39.5720	86.22388	1.2777	410.0

α (esu) = 0.148185x10^{-24} α (au)

4.3.2.1.c Hyperpolarizability (β)

Static CPHF hyperpolarizability values are summarized in **Table 4.11.** All the polymers have β values higher than that of the reference material 2-methyl-4-nitroaniline (MNA). Even for the polymer that has not been incorporated with the chiral molecule (Pol-0), the β values are almost double (186%) compared to the reference MNA. From the charge transfer perspective, this can be understood by observing the HOMO-LUMO gap (ΔE). In MNA, ΔE is 0.40 eV and that of polymers are approximately 0.34 eV. Hence, in polymers, charge transfer will occur easily compared to MNA. Thus, HOMO-LUMO gap of monomers plays a vital role in polymer design. The ΔE of chromophores is approximately 0.33 eV and that of chiral molecules is approximately 0.45eV. The co-polymer of these chromophores and chiral molecules has the ΔE approximately 0.34eV. The chromophores with good donor-acceptor capacity have

reduced the ΔE of polymers considerably. Thus, the choice of monomers with low HOMO-LUMO gap is important in designing the polymers with high SHG efficiency. All the polymers have helically oriented conformation in the optimized structure.

Table 4.11: HOMO-LUMO gap (ΔE) in eV, Ground-State Dipole Moment (μ_g) in debye, Linear Polarizability (α) in units of 10^{-23} esu, and First Hyperpolarizability (β) in units of 10^{-30} esu for the polymers (ab initio CPHF static property calculations)

Polymers	ΔE	μ_g	α	β_{vec}
Pol-I	0.3490	5.4301	11.8683	9.9628
Pol-II	0.3444	5.9517	11.8686	10.2300
Pol-III	0.3415	7.6149	11.4086	7.8581
Pol-IV	0.3511	3.7505	11.3310	10.2211
Pol-V	0.3482	5.7085	11.0709	8.8682
Pol-VI	0.3505	3.5832	11.7934	10.1684
Pol-VII	0.3433	5.0667	6.9456	12.6699
Pol-VIII	0.3429	4.5357	6.9286	12.6383
Pol-0	0.3441	3.5672	10.4122	7.5995
MNA	0.4047	6.1859	1.2777	4.0778

Figure 4.20 shows the AM1 optimized geometry of the polymer containing three repeating units. The helical structure ensures the macroscopic chirality and thus the asymmetry, basic and essential requirement for second order NLO material. All the polymers have lower ground state dipole moment than MNA. The polymers with low dipole moments could reduce the chromophore-chromophore interaction in the macroscopic assemblies related to more conventional polymeric architecture and therefore be more useful as NLO material.[39,40] Hence, with all these factors, all the designed polymers are very good materials for second harmonic generation.

While examining the effect of chiral molecule in designing an efficient SHG material, it can be seen that all the polymers (**Pol-I** to **Pol-VIII**) with chiral molecules have high β value than the polymer with out the chiral molecule (**Pol -0**). The HOMO-

LUMO gap is almost same in all the polymers. The chiral effect is clearer from the *dynamic* property calculations (**Table 4.12**).

Table 4.12: Oscillator strength (f), Optical Gap (δE) in eV, Ground-State Dipole Moment (μ_g) in debye, Difference in dipole moments between ground state and excited state ($\Delta\mu$), Linear Polarizability (α) in units of 10^{-23} esu, and First Hyperpolarizability (β) in units of 10^{-30} esu for the polymers (ZINDO-SOS dynamic property calculations)

Polymer	*f*	δE	Δμ	μ_g	β_{vec}	β_{vec}*
Pol-I	2.0588	5.1699	20.9684	41.0062	338.9870	9.9628
Pol-II	2.3105	5.2810	20.4410	43.4733	387.4365	10.2300
Pol-III	2.6603	5.4951	35.2631	32.8368	630.2270	7.8581
Pol-IV	2.6388	5.5311	36.1949	25.6171	708.5834	10.2211
Pol-V	2.5280	5.2994	23.8548	13.1032	338.5161	8.8682
Pol-VI	2.4066	5.2728	26.8567	55.6095	364.9942	10.1684
Pol-VII	0.9736	4.7253	34.0544	19.0390	479.0832	12.6699
Pol-VIII	1.0243	4.7356	33.1411	23.5745	478.5394	12.6383
Pol-0	0.2488	13.8755	9.1368	33.1546	4.2718	7.5995
MNA	1.0582	7.2925	13.7011	42.4044	202.3979	4.0778

* *Static values*

It is really surprising that in *dynamic* calculation the value of β_{vec} of the polymer without chiral molecule is very low (in two orders of magnitude) compared to the polymers with chiral molecules. It is not so pronounced in the *static* CPHF calculation due to the limitation of derivative method rather than SOS formalism. In the SOS *dynamic* calculation, contributions from all the excited levels have been taken in to account for getting the total value of β_{vec}.

For **Pol-0**, the polymer without chiral molecule, the oscillator strength (*f*), which determines the transition probability from the ground state to the excited state, is low compared to the other polymers with chiral building units. Also, the optical gap (*δE*), which determines the energy gap between the ground state and the lowest dipole allowed state, is large for **Pol-0**. Because of this very small oscillator strength and large

optical gap, charge transfer is difficult in **Pol-0** compared to other polymers. Even though, **Pol-0** has comparatively good ground state dipole moment, its difference in dipole moment between the ground state and the excited state $\Delta\mu$, is small compared to others. All these factors reduce the value of β_{vec} considerably. Thus all the chiral molecules are effective in making potential chiral NLO polymers. In MNA also, the value of δE is very high and $\Delta\mu$ is very low. But its oscillator strength is much higher than that of **Pol-0**. Hence, according to SOS calculation, MNA has more β value than **Pol-0**. It can be concluded that chirality plays a vital role in increasing the microscopic second order response of NLO material.

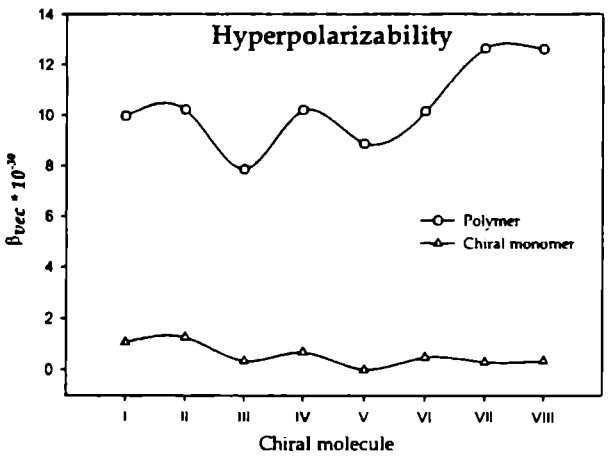

Figure 4.8. Stereochemical effect of chiral monomers and Polymers on β

The stereochemical effect of the chiral molecule has shown the same trend as predicted for the chiral monomers (**Figure 4.8**). All polymers are oriented as Λ helix. Even in this highly ordered helical structure, the stereochemistry of the incorporated chiral monomers is an important factor in determining the value of β. For each pair of polymers (incorporated with each member of the diastereomeric pair), all other properties are same except the stereochemistry of the chiral monomer. In all polymers, the stereochemistry of azomesogen chromophores was also kept unaltered. Still, there is visible difference in the microscopic β values with respect to the stereochemistry. In the case of camphanediol pair, the polymer incorporated with exo-exo diastereomer has shown higher β value. In isosorbide-isomanide pair, the effect is more pronounced. (**Pol-III** and **Pol-IV**), and the polymer with isomanide has shown high β value. The polymers with (2R, 3S) diethyl tartrate, have also shown a good β value compared to MNA. This is because, while incorporating in to the polymer chain, the center of symmetry of the

chiral monomer has became unimportant and the two chiral centers in the molecule become active in the helical polymer chains. The (2R, 3R) diethyl tartrate has shown higher value of β in that pair. The polymers containing camphoric acid pair have not shown any visible stereochemical effect.

Table 4.13: Dipole moment difference between the ground state and excited state in units of deby and First Hyperpolarizability (β) in units of 10^{-30} esu for the polymers (ZINDO-SOS dynamic property calculations)

Polymer	$\Delta\mu_x$	$\Delta\mu_y$	$\Delta\mu_z$	$\Delta\mu$	β_{vec}
Pol-I	15.7750	-2.2028	12.8114	20.4410	387.4365
Pol-II	19.5195	4.0585	6.4955	20.9684	338.9870
Pol-III	24.8597	18.0235	17.3388	35.2631	630.2270
Pol-IV	26.6185	19.1062	15.3779	36.1949	708.5834
Pol-V	15.2025	7.2909	-16.8753	23.8547	338.5161
Pol-VI	18.0382	-11.1415	16.4855	26.8567	364.9942
Pol-VII	32.9943	-2.5501	-1.7902	33.1411	479.0832
Pol-VIII	33.7235	0.6646	-4.6877	34.0544	478.5394

In the case of polymers also, a clear picture of the effect of stereochemistry in the β_{vec} will be obtained from the $\Delta\mu$ values (**Table 4.13**). The polymers that showed higher β has also shown high value of $\Delta\mu$ and $\Delta\mu_x$ (x direction is fixed as the charge transfer direction in all optimized geometries). This stereochemical dependence of β of polymers is inherent from the stereochemistry of the incorporated chiral molecules (**Figure 4.8**). It can be concluded that the stereochemistry of the chiral molecules is very important in designing a good NLO material with high second order nonlinear response.

4.3.2.1.d Chiral component

The values of β tensors are summarized in **Table 4.14**. The β_{xyz} component of all the polymers is very large compared to MNA. In **Pol-0**, even if, the value of β_{xyz} is lower than that of other polymers (with chiral molecules), it is not negligible as in the case of MNA. The chirality of the polymers has arrived from 1) the incorporated chiral

molecules and 2) the macroscopic Λ helical structure of the polymers. Even after incorporating in to the polymer matrix, the stereochemistry of the chiral molecule is relevant in predicting the chiral tensor component, χ_{xyz}. The isosorbide system has low χ_{xyz} value than the isomanide system. To conclude, in the macroscopic structure, the contribution to the χ_{xyz} should be very large for these polymers and they will give high macroscopic SHG response.

Table 4.14: First hyperpolarizability tensors of polymers β (static) in atomic units

β *Tensors*	Pol-I	Pol-II	Pol-III	Pol-IV	PolV	Pol-VI	Pol-VII	Pol-VIII	Pol-0	MNA
β_{xxx}	-891.4448	-859.4220	-269.3773	-907.2016	-1010.94	-745.2186	226.2505	-366.8170	-246.295	562.8668
β_{xxy}	228.8973	243.8666	314.1583	187.0105	176.6139	274.8180	143.2297	138.6167	292.2001	126.1593
β_{xyy}	286.9885	292.1974	257.0262	243.5943	284.7539	273.0921	676.6643	-636.4977	244.0996	-83.3171
β_{yyy}	-385.3391	-335.5022	-350.7704	-430.1264	-429.945	-332.4573	470.9063	-418.7210	-389.542	-95.7037
β_{xxz}	290.6427	316.3345	175.5984	295.4173	269.1672	246.5883	97.4063	80.4576	140.9893	21.55855
β_{xyz}	124.4980	128.0857	103.5382	133.1641	123.8529	194.2914	119.7820	-348.5849	97.96917	-3.36694
β_{yyz}	517.8861	523.6910	469.1134	509.0435	492.3874	489.7958	689.3754	-386.9942	487.883	0.253731
β_{xzz}	187.0674	180.1087	226.9713	181.6496	199.808	188.6180	109.4226	-234.5269	205.7406	-12.592
β_{yzz}	72.2561	85.4088	103.8087	81.8387	106.3873	88.7089	-151.6933	-266.9824	93.39935	30.74238
β_{zzz}	263.2106	278.7315	236.6339	263.9292	280.8862	249.7160	168.2840	-248.9099	226.9094	9.886996
β_X	-417.3889	-387.1160	214.6202	-481.9576	-526.383	-283.5085	1012.3374	-1237.842	203.5457	466.9577
β_Y	-84.1857	-6.2268	67.1966	-161.2771	-146.944	31.0695	462.4427	-547.0957	-3.94266	61.19799
β_Z	1071.7395	1118.7571	881.3456	1068.3901	1042.441	986.1000	955.0657	-555.4465	855.7817	31.69927
β_{vec}(au)	1153.2243	1183.8560	909.5863	1183.1107	1177.011	1026.5163	1466.5711	1462.9034	879.664	472.0165
β_{vec}(esu)*	9.96289	10.230	7.8581	10.221	10.200	8.8682	12.670	12.638	7.600	4.080

β (10^{-32} esu) = 0.863916β (au)

4.4. Synthesis

A series of polymers incorporating chiral molecules are designed with the help of theoretical calculation by optimizing the stereochemical effect of the chiral molecule. The most promising ones have been synthesized and SHG efficiency was measured experimentally. One diastereomer, each from the four diastereomeric pairs, was selected for incorporation in the polymeric structure; except isosorbide-isomanide pair. Polyesters containing both isosorbide and isomanide pair were synthesized to prove the stereochemical effect experimentally. Thus, five polymers were synthesized in the laboratory incorporating chiral monomers, biphenol (**5**) and diacid chloride (**8**) by high temperature polycondensation. The chiral molecules selected were (1R, 2S, 3R, 4S)-camphanediol (exo-exo camphanediol), isosorbide, isomanide, (2R, 3R)-diethyl tartrate and (1R, 3S)-camphoric acid (D (+) or exo-exo) (**Figure 4.9**). The polyester that does not contain any chiral molecule was also synthesized. The synthetic procedures are described in the following section.

4.4.1 Monomer synthesis

4.4.1.1 Synthesis and characterization of chiral molecules

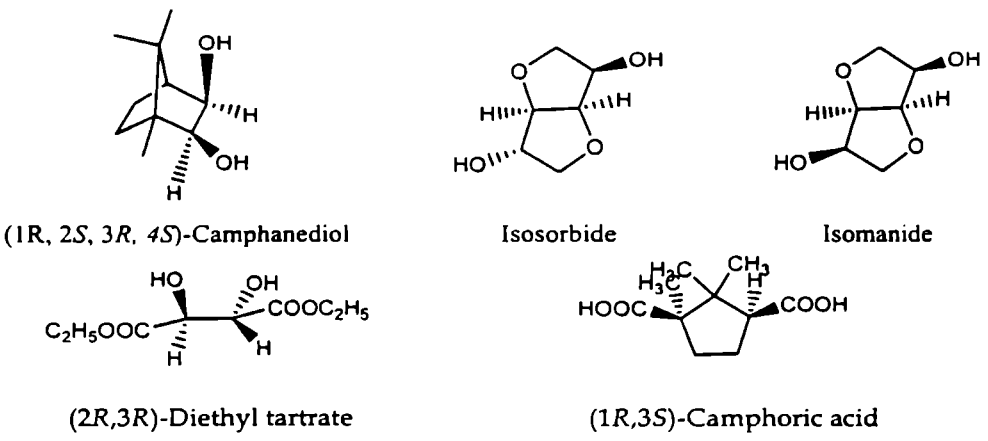

Figure 4.9. Chiral monomers used for polymer synthesis

Theoretical study of eight chiral monomers were done and out of which five chiral molecules (**Figure 4.9**) were selected for the synthesis of polymeric systems. They

are (1R, 2S, 3R, 4S)-camphanediol (exo-exo camphanediol), isosorbide, isomanide, (2R, 3R)-diethyl tartrate and (1R, 3S)-camphoric acid (D (+) or exo-exo). Isosorbide (Lancaster, 98% pure), isomanide (Fluka, 98% pure), (2R,3R)-diethyl tartrate (Merck - Germany, 97% pure) and (1R,3S)-camphoric acid (D(+) or exo-exo) (Lancaster, 98% pure) were commercially available. (1R, 4S) camphanediol (exo-exo) was synthesized from camphoroquinone.

Synthesis of (1R, 4S)-(-)- camphoroquinone[41,42]

SeO_2 (s. d. fine 99% pure), D (+) camphor (Lancaster, 97% pure), acetic anhydride (E.Merck, G.R) were used as starting materials for synthesizing camphoroquinone. Unless otherwise specified all other reagents, through out the synthesis, were of analytical grade and all the chemicals were used as obtained.

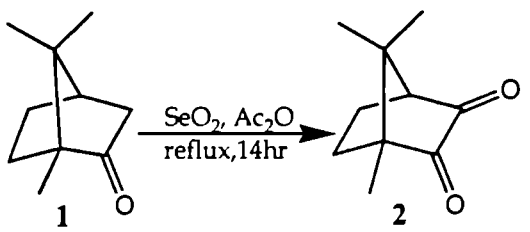

1 2

Scheme 4.1. Synthesis of camphoroquinone

Synthetic procedure: (D) (+) camphor **1** (20.0g 0.13 mol) was taken in a 125mL three necked, round-bottom flask fitted with a reflux condenser with stirring. Selenium dioxide (8.0 g, 0.07 mol) and reagent grade acetic anhydride (14 mL) was added to it. The green solution was stirred at reflux for 1 h, cooled to ambient temperature, and an additional amount of selenium dioxide (8.0 g, 0.07 mol) was added. The mixture was again heated to reflux, and two further batches of selenium dioxide (8.0 g, 0.07 mol) were added at 2.5 h and 6 h intervals. The reaction mixture was heated at reflux for an additional 8 h, during which time, precipitation of selenium metal was observed. It was cooled to ambient temperature and transferred to 125 mL beaker with the aid of 50 mL of ethyl acetate and the solution was filtered by applying vacuum. The filtrate was transferred to a 1-L separating funnel and was washed successively with 10% aqueous sodium hydroxide (200 mL) solution and saturated aqueous sodium chloride (100 mL)

solution. The organic layer was separated and dried over anhydrous magnesium sulphate, filtered and concentrated to get crude (1R,4S) (-) camphoroquinone (**2**) as yellow crystals. It was recrystallised from a mixture of hexane and 2-propanol. (**Scheme 4.1.**) This material was used for the synthesis of (1R, 4S) (+) exo-exo 2, 3- camphanediol.

Characterization

Yield 84.5%, $[\alpha]_D$ = -107.4 (c=10mg/ml in DMF). M.P 198-199^0 C (lit. mp 199^{0}C) [41]

Elemental analysis: Calculated for $C_{10}H_{14}O_2$ - C, 72.26; H, 8.49; O, 9.25. Found - C, 72.20; H, 8.55; O,9.30

Spectral properties

UVλ_{max} nm :430

IR(KBr pellet) cm^{-1} : 1767 and 1746 (α diketone ,aliphatic six membered ring), 994 (=CH)

^{1}H NMR (300 MHz $CDCl_3$): δ 1.03 (s, 3H, bridge head methyl), 1.11 (s,3H, bridge head CH_3), 1.27 (s, 3H, bridgehead CH_3), 1.88 (m,2H, ring CH_2), 1.75 (m,2H, ring CH_2) 2.35 (m, 1H, bridge head -CH)

^{13}C NMR (75 MHz $CDCl_3$): δ 15.9 (-CH_3 aliphatic), 22.1 (CH_3, aliphatic) 22.4 (-CH_3 aliphatic), 22.8 (-CH_2, cyclopentane), 31.8 (-CH_2, cyclopentane), 37.7 (-C, cyclopentane) 54.3 (-C, cyclopentane), 55.2 (-CH, cyclopentane), 202(-C, carbonyl), 207.6 (-C, carbonyl)

Mass (m/z) : molecular ion peak at = 166, 28 (-CH_2-CH_2-), 43 (-CH_2-C=O)

IR peaks at 1767 and 1746 cm $^{-1}$ are characteristic of α diketones in six membered ring system. ^{1}H NMR peak at δ 2.35 implies the presence of camphor bicyclic ring ketone. Peaks at δ = 22.8, 31.8 ,37.7 in ^{13}C NMR are characteristic of camphor bicyclic ring system. δ = 202 and 207.6 are due to six memebered ring carbonyl group.

Synthesis of (1R, 2S, 3R, 4S)-camphanediol

$LiAlH_4$ (Aldrich, 95% pure) was used for reduction. Extremely dry ether was obtained by benzophenone ketyl procedure.[43,44]

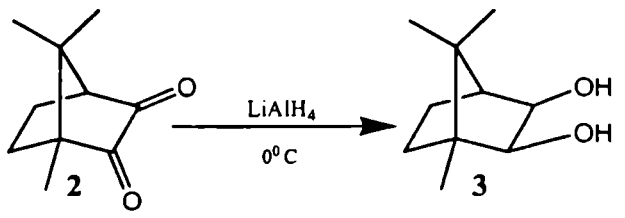

Scheme 4.2. Synthesis of (1R, 2S, 3R, 4S)-camphanediol

Synthetic procedure: Camphoroquinone (**2**) (30 g, 0.18 mol) in dry ether (360 mL) was taken in a 500mL beaker kept in an ice bath. $LiAlH_4$ (98g, 2.5 mol) suspended in dry ether (100 ml) was added to it. After an exothermic reaction, the mixture was kept at 0^0 C for further 20 min. and refluxed for 1 h. The excess amount of $LiAlH_4$ was decomposed with 0.5 M sulphuric acid in an ice bath. The reaction mixture was washed several times with dil. sodium hydroxide and dried over anhydrous magnesium sulphate to get crude (1R, 4S)(+) exo-exo 2,3- camphanediol as white solid (**3**). This solid was recrystallized from dry ether and sublimed at 110^0 C (**Scheme 4.2.**)

Characterization

Yield 86%, $[\alpha]_D = -12^0$ (c=10mg/ml in dry ether).

Elemental analysis: Calculated for $C_{10}H_{18}O_2$ - C, 70.55; H, 10.66; O, 18.79. Found - C, 70.69; H, 10.51; O, 18.80

Spectral properties

UVλ_{max} (nm): 315

IR(KBr pellet) cm^{-1} : 1364, 1390(*gem*-dimethyl group, symmetric and asymmetric C-CH_3 stretching),3230 (-OH stretching)

^{1}H NMR (300 MHz $CDCl_3$): δ 7.25 (-OH), 3.55-4.05 (-CH, 2 & 3), 2.25- 2.65 (-CH, 4), 1.4-1.8 (-CH_2, 5 & 6), 0.85-1.15(-bridge head CH_3 8 & 9), 0.75-0.84 (bridge head CH_3, 10)

^{13}C NMR (75 MHz $CDCl_3$): δ 79.89, 77.38 (C2), 76.13-77.05 (C3), 48.97, 51.55 (C4), 46.45, 48.76 (C1), 45.12, 46.33 (C7), 38.99, 40.45 (C6), 33.99-24.12 (C8 & C9), 21.86, 21.04 (C5), 20.46, 20.11 (C10)

Mass (m/z) 170 (molecular ion), 169 ($M^+ - H^-$), 152 ($M^+ - H_2O$), 141 ($[M-1]^+$ -CO), 42(-$C(CH_3)$,

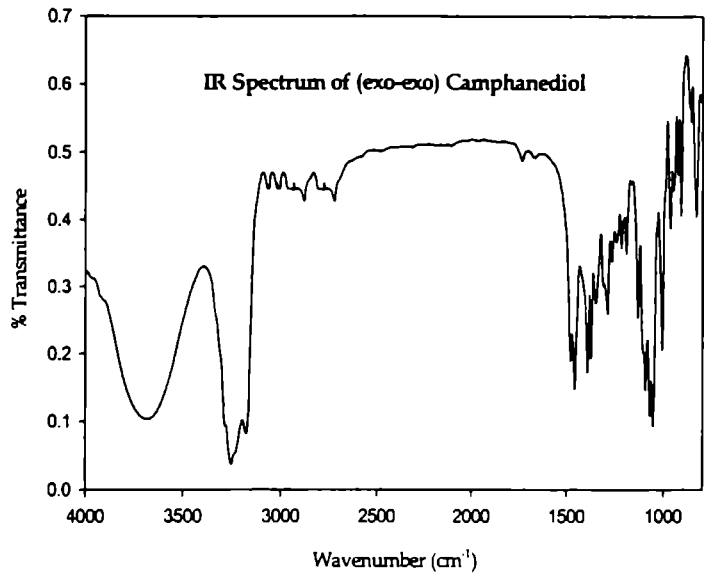

Figure 4.10. IR Spectrum of (exo-exo) Camphanediol

The IR spectrum of exo-exo camphanediol shows a complexity in the 1373-833 cm^{-1} region typical of many stretching and bending vibrations present in organic compounds. Since camphanediol contains a *gem*-dimethyl group [$(CH_3)_2$ C] the spectrum displays a sharp doublet at 1364 and 1390 cm^{-1}

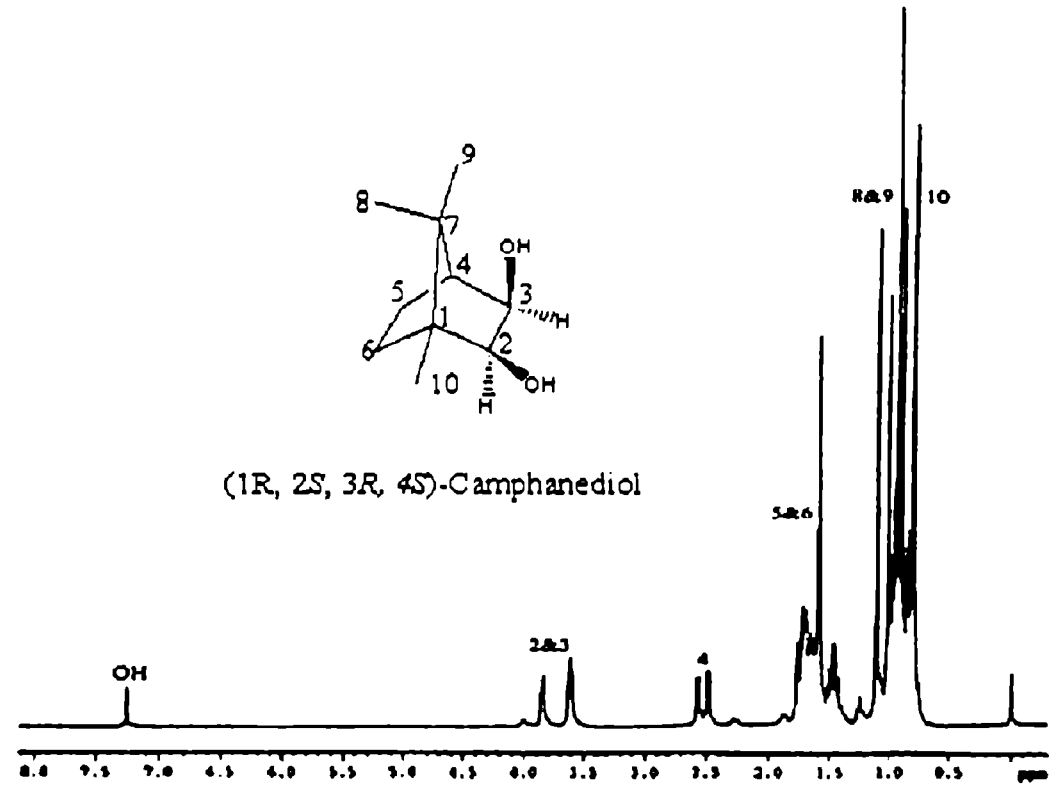

Figure 4.11. ^1H NMR of Camphanediol

The ^{1}H NMR and ^{13}C NMR spectra of camphanediol are complex spectra due to spin spin coupling. Because the bicyclic bridged system is a strained ring system, coupling exists between all most all the protons and also between the carbons. The -OH peak at δ 7.5 confirmed the reduction of camphoroquinone into camphanediol. The absence of peaks after δ 100 confirmed that there is no more carbonyl carbon in the compound. -OH carbons appeared at δ 79.89 and 76.13. The mass spectrum also confirmed the proposed structure.

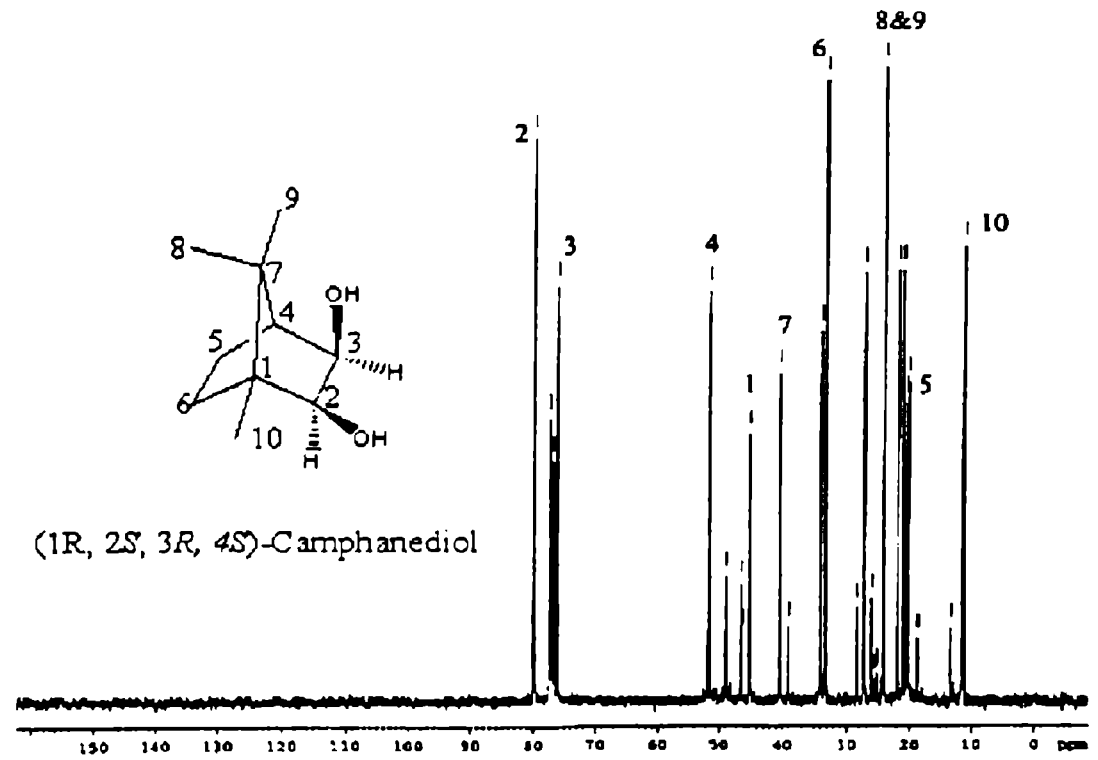

Figure 4.12 ^{13}C NMR of Camphanediol

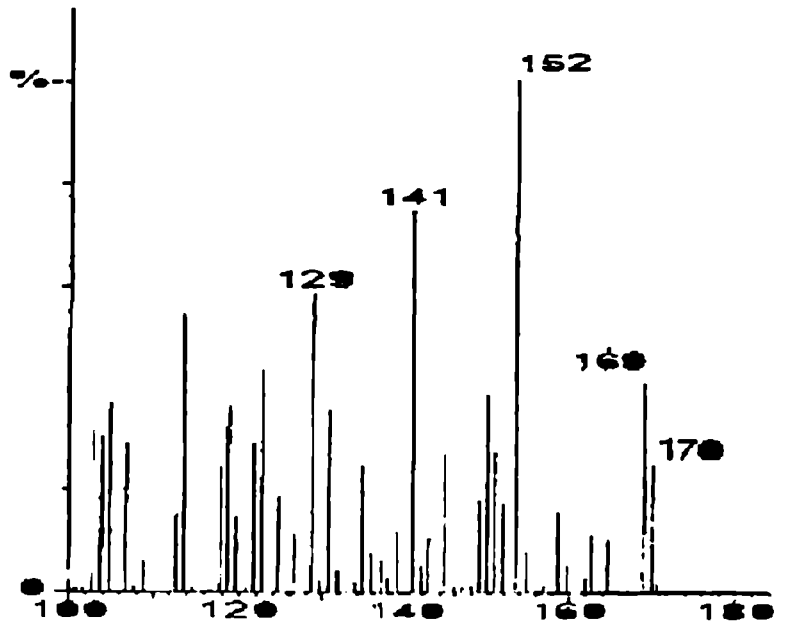

Figure 4.13 ESI mass spectrum of Camphanediol

4.4.1.2 Synthesis and characterization of chromophores

The selected chromophores, bis(4-hydroxyphenylazo)-2,2′-dinitrodiphenyl methane (BHDM) and azobenzene-4,4′-dicarbonyl chloride (AZCl) were synthesized according to the standard procedures. *B*is(4-hydroxyphenylazo)-2,2′-dinitrodiphenylmethane (BHDM) was synthesized from 4,4′-diamino-2,2′-dinitrodiphenylmethane.[16] Both are azo benzene compounds. Derivatives of azo-benzene compounds containing donor-acceptor groups have been widely exploited as NLO chromophores in polymeric systems.[45-48] The synthesis of these compounds can be easily accomplished by a diazo coupling reaction. Diazo coupling reaction is the first reported reaction for the synthesis of azo benzene compounds and it is the single most used reaction for the synthesis of azo dyes till date. This electrophilic substitution reaction leads to regioselectivity and usually a high yield of the product. The reaction involves coupling between a diazotized aromatic amine and a coupling component such as phenol, naphthols, aromatic amines and active compounds.[49] The regioselectivity of diazo coupling reaction leads to the preferential formation of the *para* isomers. There are

two geometrical isomers known for azo benzene derivatives named *cis* and *trans* (**Figure 4.14**). Among these the *trans* is more stable but *cis* is naturally occurring. [50]

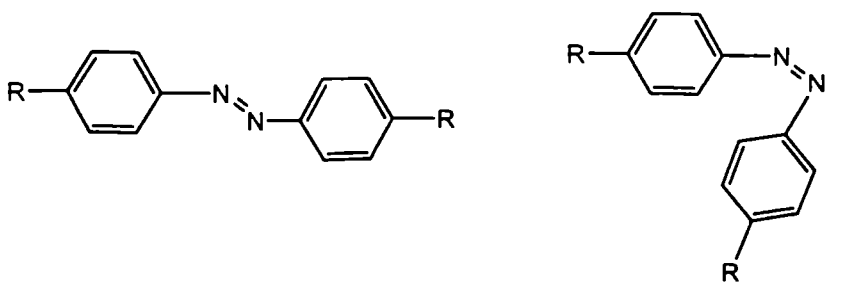

Trans form Cis form

Figure 4.14. Geometrical isomers of azobenzene derivatives

4.4.1.2.1 Synthesis of 4, 4'-diamino-2,2'-dinitrodiphenylmethane

4, 4'-diaminodiphenylmethane (Lancaster 97% pure), Potassium nitrate (s. d. fine. 99% pure) were used for the synthesis of bis(4-hydroxyphenylazo)-2,2'-dinitrodiphenylmethane (BHDM).

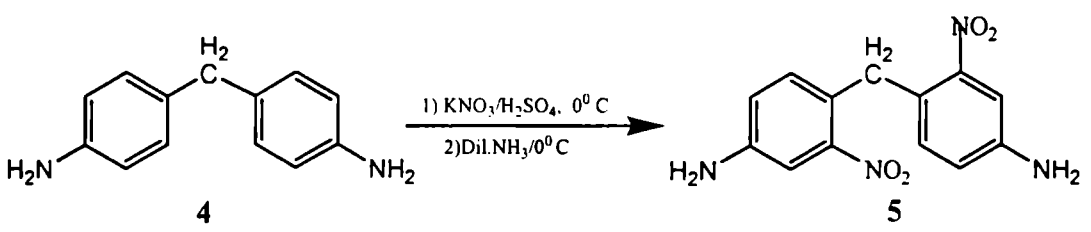

4 5

Scheme 4.3. Synthesis of 4, 4'-diamino-2,2'-dinitrodiphenylmethane

Synthetic Procedure: 4, 4'-Diaminodiphenylmethane (4) was nitrated using a mixture of anhydrous potassium nitrate and 98% sulphuric acid. 500 mLbeaker was placed in a 0^0 C ice bath with magnetic stirring. It was charged with an ice cold solution of 4,4'-diaminodiphenylmethane (10g, 0.05 mol) in conc. sulphuric acid (40 mL, 18M). To this solution, potassium nitrate solution (10g, 0.1 mol) in conc. sulphuric acid (15 mL, 18 M) was added drop wise during a period of 1h, using a dropping funnel. The stirring was continued for 3 h, keeping the temperature below 5^0 C. The reaction mixture was poured in to crushed ice and neutralized with ice cold solution of ammonia. The orange-yellow solid was collected by filtration, washed thoroughly with water. Crystallization from a mixture of dioxane-alcohol afforded orange-yellow flakes of 4, 4'-diamino-2,2'-

dinitrodiphenylmethane. This was used for the synthesis of bis(4-hydroxyphenylazo)-2,2'-dinitrodiphenylmethane (BHDM) (**5**) (**Scheme 4.3.**)

Characterization

Yield 89.6%. M.P. 205^0 C

Elemental analysis: Calculated for $C_{13}H_{12}N_4O_4$ - C, 54.14; H, 4.16; N, 19.44. O, 22.26 Found - C, 54.11; H, 4.18; N, 18.80; O, 22.91

Spectral properties

UVλ_{max} nm : 308 (NO_2)

IR(KBr pellet) cm^{-1} : 1540, 1350 (NO_2)

^{1}H NMR (300 MHz $CDCl_3$): δ 4.8 (s, 4H, -NH_2), 8.2 (s, 2H,aromatic), 7.6 (d, 2H aromatic), 7.3 (d, 2H, aromatic), 5.0 (s, 2H -CH_2)

^{13}C NMR (75 MHz $CDCl_3$): δ 34 (-CH_2), 118, 124,130, 135, 147, 157 (aromatic)

The 4, 4'-diaminodiphenylmethane (**4**) was nitrated using potassium nitrate and concentrated sulphuric acid, according to a reported procedure.[51] In 98% sulpuric acid, nitration takes place at the meta position of NH_3^+group. The dinitro derivative (**5**) was reported earlier.[51] Peaks at 1350 and 1540 cm^{-1} confirmed the nitro substitution. The elemental analysis of the compound confirmed diniration of (**4**). In ^{13} C NMR spectra of (**5**) there were only six peaks corresponding to aromatic hydrogens. So the nitro substitution in both the nuclei was symmetrical. Also in ^{1}H NMR spectra, the absence of singlet peak at or above δ 8.9 showed that there was no aromatic hydrogen *ortho* to nitro groups or the nitro group was substituted in the meta position of the amino group.

4.4.1.2.2 Synthesis of bis(4-hydroxyphenylazo)-2,2'-dinitrodiphenylmethane (BHDM)

Sodium nitrite (s. d. fine 98%), Phenol (E. Merck, 99%) were used for the synthesis of bis(4-hydroxyphenylazo)-2,2'-dinitrodiphenylmethane (BHDM) (**5**).

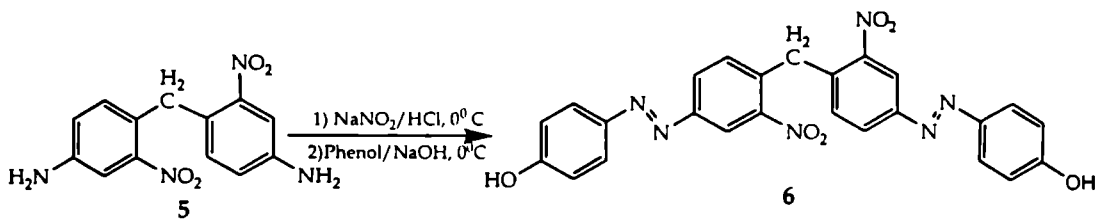

Scheme 4.4. Synthesis of bis(4-hydroxyphenylazo)-2,2'-dinitrodiphenylmethane

Synthetic Procedure: An ice cold solution of 4, 4'-diamino-2, 2'-dinirtodiphenylmethane (5) (10g, 0.035 mol) in hydrochloric acid (20 mL, 6M) was taken in a 500 mL beaker. The solution was kept under magnetic stirring. To this solution, cold aqueous sodium nitrite solution (6 g in 15mL of H_2O) was added drop wise from a dropping funnel. The diazonium salt was obtained as yellow solution. This diazonium salt was added to a cold alkaline solution of phenol (6.58 g, 0.07 mol). The resulting solution on acidification yielded a brown solid (6). It was collected by vacuum filtration, washed with water, dried and purified on a silica gel column using benzene and benzene-ethyl acetate mixture. (**Scheme 4.**)

Characterization:

Yield : 70%. M.P: 252^0 C

Elemental analysis: Calculated for $C_{25}H_{18}N_6O_6$ - C, 60.24; H, 3.64; N, 16.86. O, 19.26 Found - C, 60.18; H, 3.58; N, 16.76; O, 19.48

Spectral properties

UVλ_{max} nm : 308 (NO_2), 375 (-N=N-)

IR (KBr pellet) cm^{-1} : 3400 (-OH), 1540, 1345 (NO_2), 1453 (-N=N-)

^{1}H NMR (300 MHz $CDCl_3$) δ : 5.1 (s, 2H, -CH_2), 7.3 (d, 2H, aromatic), 7.7 (d, 2H, aromatic), 7.8 (d, 2H, aromatic), 8.5 (d, 2H, aromatic), 8.7 (s, 2H, aromatic), 9.9 (s, 2H - OH)

^{13}C NMR (75 MHz $CDCl_3$) δ : 34 (-CH_2) 117, 119, 124, 128, 136, 139, 142, 150, 152 and 154 (aromatic)

The peak at 3400 cm^{-1} in the IR spectrum and a singlet peak at δ 9.9 in the ^1H NMR spectrum are due to hydroxyl groups. The peak between 375 and 380 nm in UV-Vis absorption spectrum is due to the azo group ($\pi \rightarrow \pi^*$)

4.4.1.2.3 Synthesis of azobenzene-4,4'-dicarbonyl chloride (AZCl) [52]

4-Nitrobenzoic acid (Lancaster, 95% pure), Sodium hydroxide (s d fine, 97%), Glucose (BDH, 99% pure) , Potassium carbonate (BDH, 99% pure), thionyl chloride (s. d. fine, 98% pure) were used for the synthesis.

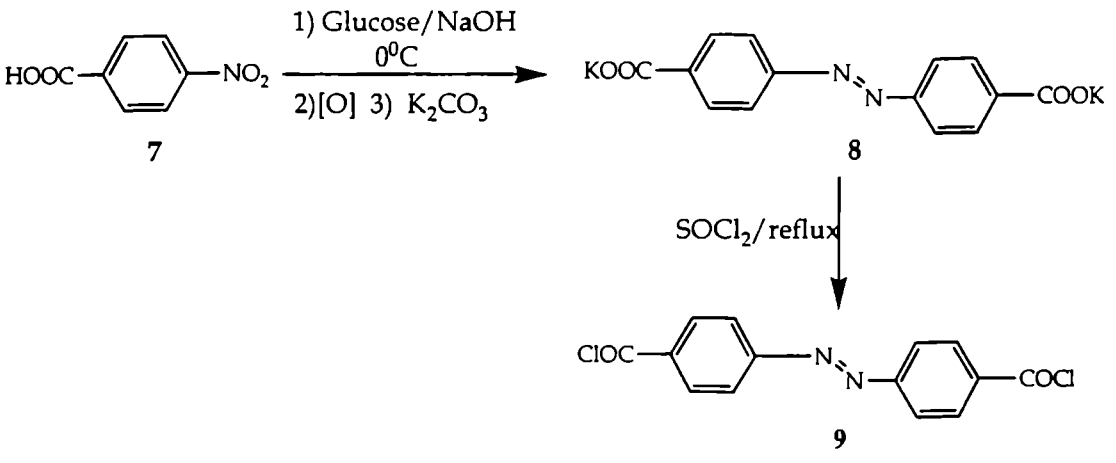

7 8 9

Scheme 4.5. Synthesis of azobenzene-4,4'-dicarbonyl chloride

Synthetic procedure: Azobenzene-4,4'-dicarbonyl chloride was synthesized according to a modified procedure of Tomlinson.[52] A two necked round bottom flask was equipped with magnetic stirring. The flask was charged with a solution of *p*-nitrobenzoic acid (7) (13 g, 0.0778 mol), sodium hydroxide (50g, 1.25 mol) and water (225 mL). To this magnetically stirred solution at 50^0 C, was added a solution of glucose (100g, 0.555 mol) in water (150 mL) over a 1 h period using pressure-equalizing funnel. The mixture was warmed on a steam bath until a yellow precipitate was formed. It was then removed and well shaken until the precipitate was dissolved to give a brown solution. A stream of air was drawn through the brown solution for 12 h, using an air blower. The mixture was slowly acidified with glacial acetic acid to pH 6 and a mud like precipitate was collected by filtration. This solid was crystallized from petroleum ether. The product was dissolved in potassium carbonate solution and recrystallisation yielded the potassium

salt of the compound. Bright orange crystals of potassium salt of azobenzene-4, 4'-dicarboxylic acid was obtained (**8**). This salt was refluxed with freshly distilled thionyl chloride for 24 h. The product was crystallized from petroleum ether to obtain red needles of azobenzene-4,4'- dicarbonyl chloride (**9**). (**Scheme 4.5.**)

Characterization

Yield: 80%. M.P: 164^{0}C

Elemental analysis : Calculated for $C_{14}H_8N_2O_2Cl_2$ C, 54.75; H,2.63; N, 9.12, Cl, 23.09, O, 10.41. Found- C, 54.72; H, 2.70; N,9.10; Cl, 23.10; O, 10.38.

Spectral analysis

UVλ_{max} nm: 330 (-N=N-)

IR(KBr pellet) cm^{-1} : 793 (C-Cl), 985 (C-CO), 1780 (C=O), 1450 (-N=N-)

^{1}H NMR (300 MHz $CDCl_3$) : δ (d, 7.9 aromatic), 8.1 (d, aromatic)

^{13}C NMR (75 MHz $CDCl_3$) : δ 122,130, 133,151 (aromatic) 168 (carbonyl)

Peak at 793 cm^{-1} in the IR spectrum indicates the presence of C-Cl bond. Peak at δ 168 in the ^{13}C NMR spectrum implies the presence of carbonyl carbon

4.4.2 Polymer synthesis

From the polymer structure designed earlier, **Pol-0, Pol-II, Pol-III, Pol-IV, Pol-VI, and Pol-VIII** have been synthesized through polycondensation of the chiral molecules and chromophores.

4.4.2.1 Optimization of reaction conditions

Table 4.15: Synthesis of Pol-0 under various conditions

Solvent	*Time (h)*	*Temp(^{0}C)*	*Yield (%)*
DMAc	25	60	45
DMAc	25	120	75
DMAc	25	160	85
DMAc	50	160	88
DMF	50	160	73
DMSO	50	160	68

The optimum conditions for the synthesis of polymers were determined by varying the temperature, time of reaction and solvent. Chiral monomer, (1R, 4S) exo-exo 2,3- camphanediol was taken for optimizing the reaction conditions (**Pol-II**) Polyesters, **Pol-0 Pol-**

II, Pol-II.a, Pol-II.b and **Pol-II.c** were synthesized according to the general procedure shown in **Schemes 6 & 8** **Pol-0** was synthesized from bis-(4-hydroxyphenylazo)-2,2'-dinitrodiphenylmethane (**6**) and 4,4'-azobenzene dicarbonyl chloride(**9**). **Pol-II, Pol-II.a, Pol-II.b** were synthesized from (1R, 2S, 3R, 4S)-camphanediol (**3**), bis-(4-hydroxyphenylazo)-2,2'-dinitrodiphenylmethane (**6**) and 4,4'-azobenzene dicarbonyl chloride (**9**) in the presence of extremely dry pyridine (s. d. fine, spectroscopic grade) as an acid acceptor in the solvent dimethyl acetamide. **Pol-II.c** was synthesized from 4,4'-azobenzene dicarbonyl chloride and (1R, 2S, 3R, 4S)-camphanediol (**3**). The optimum conditions for synthesis of the above polyesters were determined from the synthesis of **Pol-0** and **Pol-II** by a series of experiments by changing temperature, reaction time and solvent. The results are summarized in **Table 4.15.** and **Table 4.16.**

Table 4.16: Synthesis of Pol-II under various conditions

Solvent	*Time (h)*	*Temp(°C)*	*Yield(%)*	$[\alpha]_D$
DMAc	25	60	50	-5.50
DMAc	25	120	72	-7.70
DMAc	25	160	86	-10.30
DMAc	50	160	87	-35.10
DMF	50	160	65	-24.50
DMSO	50	160	70	-30.80

For **Pol-II,** the variation of temperature in DMAc medium showed that the polyester of high specific rotation in good yield was obtained at 160° C. The low value of [α] at low temperatures may be due to low percentage incorporation of (1R, 2S, 3R, 4S)-camphanediol units. An increase in reaction time from 25 h to 50 h showed only slight increase in [α] and yield. The reaction was also repeated in DMSO and DMF. But the yields and specific rotation were low. So optimum condition for the synthesis of polymers incorporating chiral unit, (1R, 2S, 3R, 4S)-camphanediol was fixed as 25 h stirring of corresponding monomers in DMAc at 160°C. For **Pol-0,** the yield increased with increase in temperature. The experiments were also repeated in DMSO and DMF but the yields were relatively low. The increase of reaction time from 25 h to 50 h showed only a nominal change in yield. So optimum condition for synthesis of **Pol-0** and **Pol-II, Pol-II.a, Pol-II.b, Pol-II.c** was fixed as 25 h stirring of the corresponding monomers in DMAc medium at 160° C.

4.4.2.1. Synthesis and characterization of Pol-0, Pol-II, Pol-II.a, Pol-II.b, Pol-II.c,

4,4'-azobenzene dicarbonyl chloride(**9**) was dissolved in extremely dry dimethyl acetamide (HPLC grade, s. d. fine). To this solution was added appropriate mole percentage of (exo-exo) camphanediol (**3**) and bis(4-hydroxyphenylazo)-2,2'-dinitrodiphenylmethane (**4**). Few drops of extremely dry pyridine (99.99% dry pyridine, s. d. fine) were added as acid acceptor. The mixture was heated under stirring for 25h at 160^0 C. The product was precipitated from cold methanol and washed continuously with hot water, methanol and acetone. After filtration and drying a brown solid was obtained.

Pol-0: 4,4'-azobenzene dicarbonyl chloride (0.01 mol, 3.06 g) and bis(4-hydroxyphenylazo)-2,2'-dinitrodiphenylmethane (0.01 mole, 4.98 g) were reacted. **(Scheme 4.6.)**

Characterization

Yield 82 %

Spectral analysis

UVλ_{max} nm : 362 ($\pi \rightarrow \pi^*$, N=N), 320 ($n \rightarrow \pi^*$, NO_2)

IR(KBr pellet) cm^{-1} : 1760 (C=O, str, ester) 1345, 1530 (N-O str, NO_2).

^{1}H NMR (300 MHz DMSO-d_6): δ 8.9-7.3 (d, aromatic), 5.3 (s, methylene)

^{13}C NMR (75 MHz DMSO-d_6): δ 172 (ester carbon), 34 (methylene carbon), 124-157 (aromatic ring carbons)

Pol-II.a: 4,4'-azobenzene dicarbonyl chloride (0.01 mole, 3.06g), bis(4-hydroxyphenylazo)-2,2'-dinitrodiphenylmethane (0.0075 mole, 3.74 g) and (exo-exo) camphanediol (0.0025 mole, 0.425 g) were reacted.

Yield: 88 %

Pol-II: 4,4'-azobenzene dicarbonyl chloride (0.01 mole, 3.06g), bis(4-hydroxyphenylazo)-2,2'-dinitrodiphenylmethane (0.0050 mole, 2.49 g) and (exo-exo) camphanediol (0.005 mole, 0.85 g) were reacted.

Yield: 83 %

Pol-II.b: 4,4'-azobenzene dicarbonyl chloride(0.01 mol, 3.06g), bis(4-hydroxyphenyalazo)-2,2'-dinitrodiphenylmethane (0.0025 mole, 1.25 g) and (exo-exo) camphanediol (0.0075 mole, 1.275 g) were reacted.
Yield: 79%

Characterization

The spectral patterns of **Pol-II.a, Pol-II, Pol.II.b** were similar

Spectral analysis

UVλ_{max} nm : 360 ($\pi \rightarrow \pi^*$, N=N), 322 ($n \rightarrow \pi^*$, NO_2)

IR(KBr pellet) cm^{-1} : 1760-1750 (C=O str. Ester formed by phenolic unit), 1735-1720 (C=O str. ester formed by camphanediol), 1520-1530 (N-O str., NO_2), 1350-1373(C-NO_2), 1610-1620 (-N=N-), 1219-1224 (doublet, $C(CH_3)_2$ of camphanediol), 2900-3000 (C-H stretch in camphanediol

^{1}H NMR (300 MHz, DMSO-d_6) : δ1.25 (s, bridged -$C(CH_3)_2$ of camphanediol), 2.1 (s, -CH_3 of camphanediol), 2.5 (m, -CH, cyclopentane ring of camphanediol), 3.0 (m, -CH_2 cyclopentane ring of camphanediol), 5.4-5.8 (m, proton near to camphanediol ester group), 6.4 (s, -CH_2), 7.6-8.9 (m, aromatic)

^{13}C NMR (75 MHz, DMSO-d_6): δ 170-175 (C of ester formed by phenolic unit), 167-164 (C of ester formed by camphanediol unit), 124-156 (aromatic carbons), 20-25 (bridge head methyl carbons in camphanediol), 40-55 (bridge head C and bridge head -CH), 37 (ethylene carbon), 75 (C adjacent to ester group)

Pol-II.c: 4,4'-azobenzenedicarbonyl chloride (0.01 mol, 3.06 g) and (exo-exo) camphanediol (0.01 mole, 1.7 g) were reacted.

Characterization

Yield: 81 %

Spectral analysis

UVλ_{max} nm : 365 ($\pi \rightarrow \pi^*$, N=N)

IR (KBr pellet) cm^{-1} : 1720 (C=O, str, ester formed by camphanediol), 1219-1224 (doublet, $C(CH_3)_2$ of camphanediol), 2900-3000 (C-H stretch in camphanediol)

^1H NMR (300 MHz DMSO-d_6) : δ 7.7, 7.8 (d, aromatic), 1.24 (s, bridged $-C(CH_3)_2$ of camphanediol), 2.1 (s, $-CH_3$ of camphanediol), 2.4 (m, -CH, cyclopentane ring of camphanediol), 3.1 (m, $-CH_2$ cyclopentane ring of camphanediol), 5.6 (m, proton near to camphanediol ester group)

^{13}C NMR (75 MHz DMSO-d_6) δ: 166 (ester carbon), 120-128 (aromatic ring carbons), 20,23,25 (bridge head methyl carbons in camphanediol), 41, 42, 45 (bridge head C and bridgehead -CH), 75 (C adjacent to ester group)

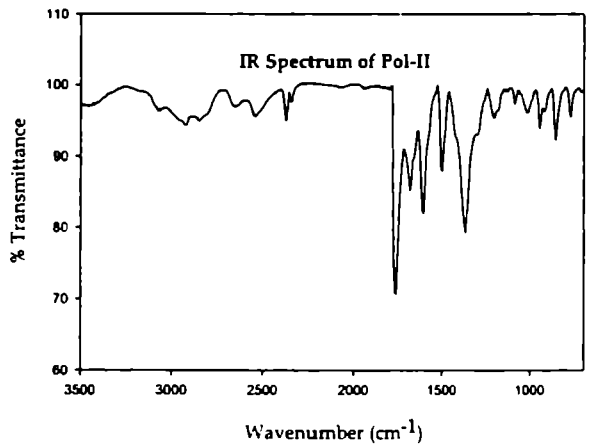

Figure 4.15. IR Spectrum of Pol-II

The polyester, **Pol-0** showed only one ester carbonyl peak between 1755-1760 cm^{-1} due to the ester bonds formed by phenolic units. But polyesters **Pol-II.a, Pol-II, Pol-II.b** showed additional peak in the region 1720-1730 cm^{-1}. This peak can be attributed due to the ester bonds formed by camphanediol units. **Pol-II.c** showed only one ester peak at 1720 cm^{-1}. In the case of ester bonds formed by camphanediol unit, there is a benzene ring adjacent to the carbonyl carbon which decreases the C=O bond order by conjugation. This decreases the frequency of C=O str. from the normal value of 1760 cm^{-1} to 1720- 1730 cm^{-1}. In the ester bond formed by a phenolic unit, there is a phenyl group attached to oxygen, which can prevent conjugation and the bond order is retained. So the carbonyl peak appears at the normal position, 1760 cm^{-1}. From the absorbance of the peaks corresponding to the carbonyl vibration between 1750-1755 cm^{-1} and 1720-1730 cm^{-1}, the ratio of chromophore and chiral unit in the polymer was determined. The analysis showed that there is only slight difference between target composition and measured composition. The

incorporation of camphanediol units was also indicated by the peaks in the region 1219-1224 cm^{-1} (doublet, $C(CH_3)_2$ of camphanediol), which is characteristic of *gem*-methyl group and 2900-3000 (C-H stretch in camphanediol).

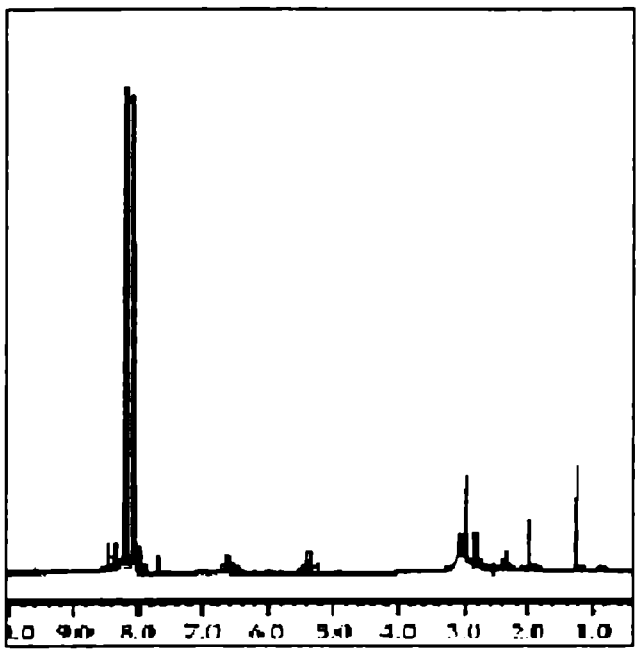

Figure 4.16. ^1H NMR spectrum of **Pol-II**

The ^1H NMR spectra of polymers showed peaks at δ 1.25 singlet due to bridged-$C(CH_3)_2$ of camphanediol, δ 2.1 singlet due to -CH_3 at bridge head of camphanediol, multiplet at δ 2.5 due to cyclohexane ring -CH of camphanediol and multiplet at δ 3.0 due to cyclohexane ring -CH_2 of camphanediol. The proton adjacent to the ester group gave multiplet between δ 5.4 and 5.8. The CH_2 protons appeared as a singlet at δ. 6.4 The absence of peaks corresponding to -OH and -COOH protons can be taken as an indication of high molecular weight. The singlet peak(s) between low field regions between δ 8.7-8.9 was due to the protons in the benzene ring *ortho* to nitro group. The peaks due to all other aromatic protons appeared as doublets between δ 7.6 and 8.4.

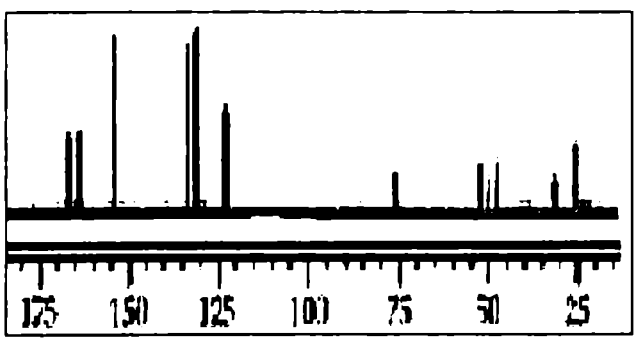

Figure 4.17. ^{13}C NMR Spectrum of **Pol-II**

The ^{13}C NMR spectrum of camphanediol containing poly-esters showed peaks at δ 25 due to bridge head methyl carbons in camphanediol (-$C(CH_3)_2$), peak at δ 30 due to -CH_3 of camphanediol, 49, 54 δ due to cyclohexane -CH_2, 60 δ due to bridge head -CH, and 75 δ due to the carbon atom adjacent to ester group. These six peaks are absent in **Pol-0**. ^{13}C NMR

spectra of polysesters other than **Pol-II.c** showed peaks between δ 170-175 due to the carbonyl carbon of ester formed by phenolic units. Polyesters containing camphanediol showed an additional carbonyl carbon peak between δ 167-164. Peaks at δ 124- 156 are due to aromatic carbon

The UV-Vis absorption spectra of the polymers were measured using diffused reflectance method of powder samples. All polymers showed the characteristic azo peak at 360-365 nm and all polymers except **Pol-II.c** showed characteristic bands due to nitro group at 320 nm. The peak positions in the UV-Vis absorption of polymers were found to be similar to those of corresponding monomers (330 and 375 nm). These results suggest that polar properties of the chromophore part is not much changed by the polymerization process.

The fairly high values for specific rotation show that no extensive racemization has occurred during polymerization stage. The [α] value increased with increase in the percentage of (1R, 2S, 3R, 4S)-camphanediol. The $[\alpha]_D$ values of the polymers were also measured after cooling from high temperature (200°C) below their decomposition temperature. There was only slight change in [α] values. This showed that the polymers even at a high temperature could retain the chiral order. The yield and properties of all polyesters are summarized in **Table 4.17.**

Table 4.17: Yield and properties of polyesters

Polymer	*Yeild (%)*	*Chiral Composition*	$[\alpha]_D$	*SHG Efficiency (MNA Reference)*
Pol-0	82	0	0	0.50
Pol-II.a	88	25	-25.0	0.88
Pol-II	83	50	-31.4	1.5
Pol-II.b	79	75	-36.8	1.1
Pol-II.c	81	100	-46.0	0.91

SHG efficiency

From **Table.4.17,** it can be seen that when the chiral loading increases SHG efficiency increases and has the maximum at 50% chiral loading. The SHG efficiency decreases with increase in chiral loading and results in a parabolic curve (**Figure 4.18**). The chirality of the polymer systems, synthesized from a polar chiral monomer and a dipolar chromophore, enhances the nonlinear optical response in two ways: first by eliminating the dipolar interactions between the chromophores which allows very high chromophore concentration, and second by chiral contributions.[8] Since both the chiral monomer and the chromophores are dipolar molecules it is necessary to optimize chiral loading according to the polar orientation. More over, the Λ shaped chromophore is the one that gives the Λ helical orientation to the polymer chain; hence, the concentration of Λ chromophore is also important here. Up to 50% chiral loading, the SHG signal increases because of the chiral contribution and decrease in dipolar interaction due to the presence of chiral molecule. After 50%, even though the chiral contribution increases, the SHG efficiency decreases due to the increase in dipolar interaction of the chiral molecules and the decrease in the possibility of attaining charge asymmetry. The decrease in the amount of big Λ shaped chromophore increases the dipolar interaction between the chiral molecules, and reduces the polar order; hence decreases the SHG efficiency.Thus for all further synthesis the chiral loading has been kept at 50%

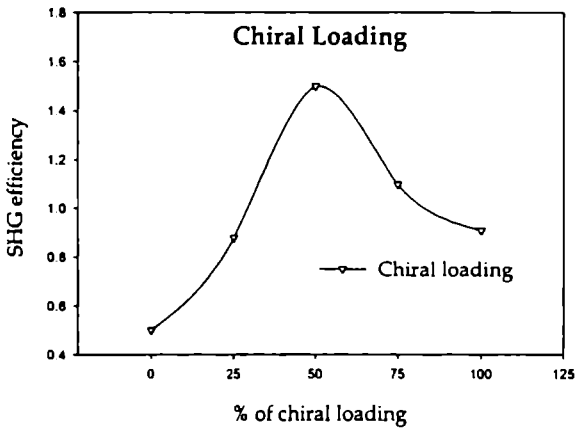

Figure 4.18 Variation of SHG efficiency with chiral loading

4.4.2.2. *Synthesis and characterization of polymers with different chiral molecules*

All polymer syntheses were done in solution method at high temperature. 4,4'-azobenzene dicarbonyl chloride (**9**) was dissolved in extremely dry dimethyl acetamide

(HPLC grade, s. d Fine). To this solution was added chiral molecule and bis(4-hydroxyphenylazo)-2,2'-dinitrodiphenylmethane (**4**). Few drops of extremely dry pyridine (99.99% dry pyridine, s. d. fine) were added as acid acceptor. The mixture was heated under stirring for 25h at 160^0 C. The product was precipitated from cold methanol and washed continuously with hot water, methanol and acetone. After filtration and drying a brown solid was obtained.

Pol-0: Synthesized according to **Scheme 4. 6. Pol II, Pol-III , Pol-IV** and **Pol-VI:** Synthesized according to **Scheme 4.8**

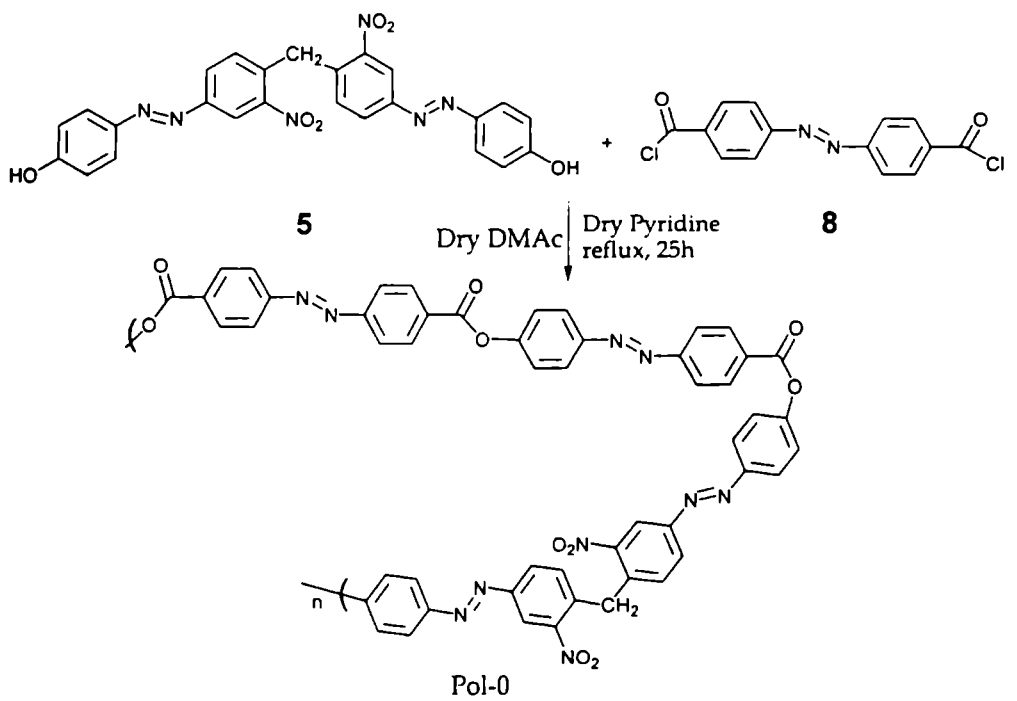

Pol-0

Scheme 4.6. Synthesis of **Pol-0**

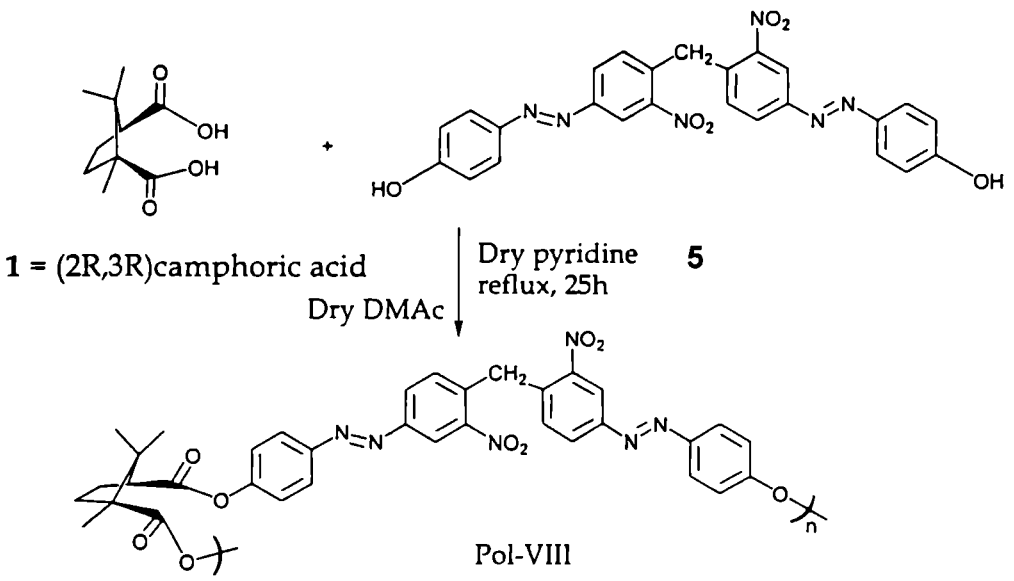

Scheme 4.7. Synthesis of **Pol-VIII**

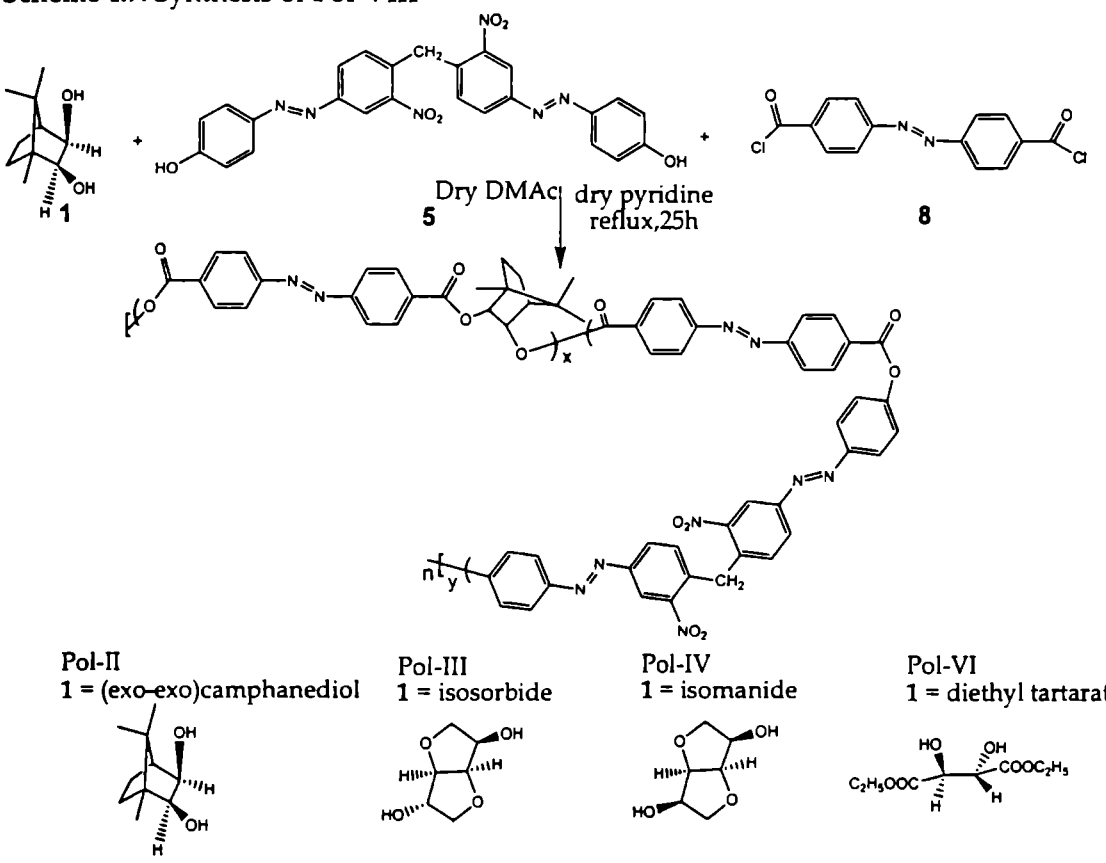

Scheme 4.8. Synthesis of **Pol-II, Pol-III, Pol-IV, Pol-VI**

Characterization was described in **section 4.4.2.1**

Characterization

Characterization of **Pol-II** was described in **section 4.4.2.1**

Pol-III (Yield 88%) and **Pol-IV** (Yield 86%) are different only in the stereochemistry of chiral monomers. So their spectral patterns are similar except in ^{1}HNMR. But in ^{1}H NMR the -CH protons which have varied stereochemistry in isosorbide and isomanide appeared as multiplets. So a distinction between them is difficult.

Spectral analysis

UVλ_{max} (solid) nm : 360 ($\pi \rightarrow \pi^*$, N=N), 322 ($n \rightarrow \pi^*$, NO_2)

IR(KBr pellet) cm^{-1} : 1760-1750 (C=O str. ester formed by phenolic unit), 1720-1735 (C=O str. ester formed by isosorbide or isomanide unit), 1520-1530 (N-O str.),1350-1373(C-NO_2), 1610-1620 (-N=N-), 2900-3000 (sp^3 -C-H stretch in isosorbide or isomanide unit), 1470-1473 (sp^3 C-H bend in isosorbide or isomanide unit), 1235-1240 (C=O str. In isosorbide or isomanide unit)

^{1}H NMR (300 MHz, DMSO-d_6) : δ 4.4 - 4.8 (m, -CH isosorbide or isomanide unit), 4.2 (q - CH_2 in isosorbide or isomanide unit), 4.0 (t, bridge CH in isosorbide or isomanide unit) 6.4 (s, -CH_2), 7.6-8.9 (m, aromatic).

^{13}C NMR (75 MHz, DMSO-d_6) : δ 171 (C in ester formed by phenolic unit), 167-164 (C in ester formed by isosorbide or isomanide unit), 124-156 (aromatic carbons), 74 (-CH_2 in isosorbide or isomanide unit), 75 (-CH in isosorbide or isomanide unit), 92 (-CH bridge in isosorbide or isomanide unit), 37 (methylene carbon).

Pol-VI

Yield -79 %

Spectral analysis

UVλ_{max} nm : 360 ($\pi \rightarrow \pi^*$, N=N), 322 ($n \rightarrow \pi^*$, NO_2)

IR(KBr pellet) cm^{-1} : 3000, 2960, 2900 (sp^3 -C-H stretch in tartrate unit), 1760-1750 (C=O str. ester formed by phenolic unit), 1725(C=O str. ester formed by tartrate), 1610-1620 (-N=N-), 1520-1530(N-O str.), 1470 (sp^3 C-H bend of CH_2 in tartrate unit), 1380 (C-H bend of CH_3 group), 1350-1373(C-NO_2).

^{1}H NMR (300 MHz, DMSO-d_6) : δ 1.2 (t, CH_3 in tartrate unit), 4.1-4.3 (q, -CH_2 in tartrate unit, 5.4 (s -CH tartrate unit), 6.4 (s, -CH_2), 7.8-8.9 (m, aromatic)

^{13}C NMR (75 MHz, DMSO-d_6): δ 174 (ester carbon in tartrate unit), 171 (C in ester formed by phenolic unit), 164 (C in ester formed by tartrate unit), 124-156 (aromatic carbons), 75 (-CH), 63 (CH_2), 37 (methylene carbon), 14 (CH_3)

Pol-VIII: was synthesized according to **Scheme 4.7.**

Characterization

Yield- 85%

Spectral analysis

UVλ_{max} (solid) nm : 361 ($\pi \rightarrow \pi^*$, N=N), 320 ($n \rightarrow \pi^*$, NO_2)

IR(KBr pellet) cm^{-1} : 1720 (C=O str. ester formed by camphoric acid unit), 1520 (N-O str.), 1350(C-NO_2), 1610-1620 (-N=N-)1219-1224 (doublet, C(CH_3)$_2$ of camphoric acid) 2900-3000 (C-H stretch in camphoric acid

^{1}H NMR (300 MHz DMSO-d_6) : δ 1.25 (s, bridged -C(CH_3)$_2$ of camphoric acid), 1.3 (s, -CH_3 of camphoric acid), 1.9-2.2 (m, -CH_2, cyclopentane ring of camphoric acid), 2.5(t, -CH cyclopentane ring of camphoric acid), 5.2 (s, -CH_2), 7.6-8.4 (m, aromatic)

^{13}C NMR (75 MHz DMSO-d_6): δ179,178 (C of ester formed by camphoric acid unit) 162, 154 (C, -CO of phenolic group) 120-156 (aromatic carbons), 53 (carbon from bridge head C(CH_3), 36 (bridge head -CH), 34, 32 (methylene from cyclopentane of camphoric acid) 30 (methylene carbon), 22 (methyl carbon from -C(CH_3)$_2$, 19 (methyl carbon from bridge head -CH_3).

Mass spectrum (**Figure 4.19**)of **Pol-IV** (m/e = 19686) equivalent to 17 repeating units (one repeating unit = 1158) is in good agreement with the proposed type of polycondensation as one repeating unit of polyester contains two diacid chloride molecule condensed with one chiral unit and one biphenol unit. The mass spectrum also gives an idea about the degree of polymerization. The high temperature polycondensation method has yielded high molecular weight polyesters

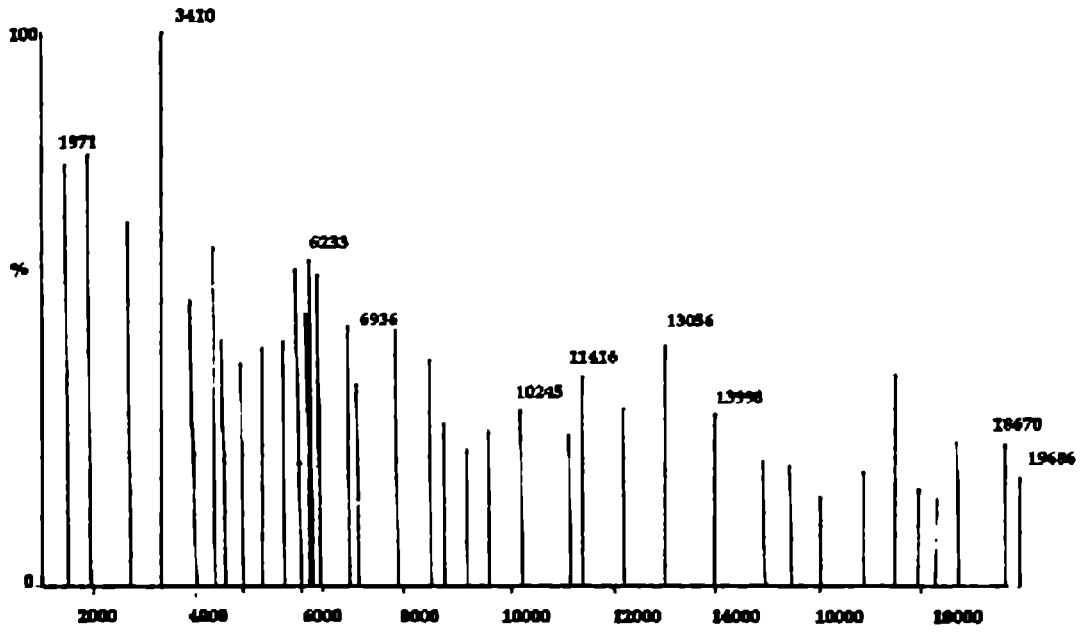

Figure 4.19 Mass spectrum of Pol-V

4.4.2.3. Thermal properties of the polyesters

Glass transition temperature of the polyesters ranges from 30-200^0 C (**Table 4.18**). Since Tg is a measure of long-range order and decrease in segmental motion in polymers, high Tg values indicate the high degree of polar order. It is interesting to note that the polymers with chiral molecules have high Tg values compared to the polymer with out chiral molecule. The introduction of chiral molecule in to the polymer main chain reduced the flexibility of polymers considerably. Also the presence of polar groups increases the Tg of the polymers. The polyesters with isosorbide (152.05^0 C), isomanide (197.84^0 C), and diethyl tartrate (138.43^0 C) have shown high Tg values which indicate that the polar ordering in these systems are really good. The camphoric acid system is also having comparably good Tg value (94.18^0 C). Even though camphanediol system has shown the lowest Tg value (52.5^0 C), it is higher than the polymer with out chiral molecule (30.3^0 C). Thus from Tg, it is very clear that incorporation of chiral molecule increases the polar ordering of the polyesters and increases the SHG efficiency. The polyester with the highest Tg values is the one that contains isosorbide or isomanide. The chiral building unit serves as a part of the chain and decreases the segmental motion considerably; hence introduce high order in the polymer chains. The stereochemical

dependence of these polymers towards polar order can be proved from the Tg values of the polymeric systems. It can be seen that the system with isomanide has shown higher Tg value than the isosorbide system. These two polymers differ each other only in the stereochemistry of isosorbide and isomanide units. The stereochemistry has played a vital role in Tg through polar ordering. Usually the system with *trans* form shows lower Tg value than *gauche* form due to the flexibility of the *trans*. Also the molecule with symmetrically ordered polar groups have low Tg value than the one with unsymmetrically placed polar group.[53] In isosorbide, the -OH groups are more symmetrically placed than isomanide. This decreases Tg of polymer containing isosorbide. From the structures of polymers containing isosorbide (**Pol-III**) and isomanide (**Pol-IV**), it can be seen that uniform stacking of isomanide polymer is very easy, because the -OH groups are oriented in the same direction; where as in isosorbide polymer, the uniform stacking is difficult due to oppositely oriented -OH groups. Thus the polymer with isomanide has more polar order and has shown higher Tg value compared with the polymers with isosorbide, in which polar ordering is reduced by the presence of oppositely oriented -OH groups. And also, the system with high polar order will show high SHG efficiency.

The initial decomposition temperature (IDT) for all polymers is above 200^0 C which indicates that all are thermally stable. The polymer with out chiral molecule has the minimum value of IDT (200^0 C) implying that the incorporation of chiral molecule increases the polymer stability also. The isomanide and isosorbide systems have higher thermal stability than other polymers. Thus from the thermal studies, it can be concluded that the polymers incorporated with heterocyclic ring systems are good systems with high Tg and IDT.

4.5. Evaluation of second harmonic generation efficiency

The NLO efficiencies of the polyesters were determined with 2-methyl-4-nitroaniline as the standard using Kurtz and Perry method.[54] Measurements were done by the powder method with a Quanta-Ray Nd:YAG laser from Spectra Physics (1064 nm, 10 ns, 365mJ/S) integrated over 20 pulse and an average of 10 pulse. The samples

were ground and graded with standard sieves to the phase matching size (100-150 μm) and loaded on cuvette with 1mm thickness. MNA samples used as standards were also powdered and sieved (100-150 μm) after drying under high vacuum. They were also mounted with the same thickness as the polymer sample. The laser beam was directed unfocused onto the sample kept at 45^0 angle to the laser beam which provided the phase matchable situation; the emission was collected from the front face of the sample at 90^0 angle. The SHG signal; at 532 nm was detected by Avantes 2048 spectrometer with CCD camera. The results are shown in **Table 4.18**.

It can be seen that all the polyesters are efficient materials for SHG. The polymer with out the chiral unit also shows SHG efficiency comparable with that of reference MNA (95%). This is because of the Λ helical structure of the polyester, due to the Λ monomer bis(4-hydroxyphenylazo)-2,2'-dinitrodiphenylmethane (BHDM) (**5**).**Figure 4.20.**

Table 4.18: Yield and Properties of Polyesters

Polymer	*Chiral monomer*	*Yield (%)*	*Tg (^0C)*	*IDT (^0C)*	*$[\alpha]_D$*	*SHG Efficiency**
Pol-II	(exo-exo) Camphanediol	83	52.5	252	-35.6	2.86
Pol-III	Isosorbide	88	152.05	278	+25.0	2.80
Pol-IV	Isomanide	86	197.84	287	+31.4	3.83
Pol-VI	(2R,3R)Diethyl tartrate	79	138.43	231	+36.8	3.07
Pol-VIII	(1R,3S) Camphoric acid	85	94.18	242	+43.9	2.99
Pol-0	With out chiral molecule	82	30.3	200	0.0	0.95

*(MNA Reference), MNA SHG efficiency =1

The polymers with chiral monomers have shown higher SHG efficiency than the reference MNA (three times greater than that of MNA). This is because of increased chirality and increased asymmetry of the polymer chains after incorporating the chiral molecules. Main chain chirality induces chemical poling, i.e., the directional orientation of the dipolar ends with out external poling. The significantly higher nonlinear optical susceptibility of the copolymers discussed in this study indicates considerable

contribution from the chirality of the polymer. Since these polymers are oriented as Λ helix, (**Figure 4.20.**), it is assumed that the copolymers have broken symmetries along the substrate normal. They therefore, belong to the symmetry group C_α; even though the monomeric units belong to C_1 point group. For such samples with C_α symmetry, there are four nonvanishing macroscopic susceptibility components; i.e, χ_{zzz}, χ_{xxz} , χ_{zxx} and χ_{xyz}. The first three components have originated from the polar ordering, while the latter can only be present in chiral media. Strong coupling exists between the chiral helical domains and the push-pull azobenzene chromophoric groups. The electron delocalisation due to the π-π* transition of the azobenzene system induces a displacement of electrons along the helical conjugated backbone. The chance for the existence of a long-range helical order in such polymer systems is rare, because, the arrangement of chiral units and chromophore units is highly random, but helical ordering (short range) is found in the polymers for the segments containing chiral units. This short range polar ordering can be proved from the high Tg values of polymers containing chiral molecules. Thus, the Λ helical structure can supplement the directional order of donor-acceptor π electron system and the dipole units are tilted in one direction along the polymer axis which leads to large values of χ_{zzz}, χ_{xxz} , χ_{zxx}, thus a high second harmonic generation efficiency. At the same time, the over all macroscopic chirality, and the chirality because of the presence of chiral monomers in the polyesters increase the value of chiral tensor χ_{xyz}. Thus chirality of the polymer systems enhances the nonlinear optical response in two ways: first by eliminating the dipolar interactions between the chromophores and second by chiral contributions.

As obtained from the theoretical calculation, to prove the stereochemical effect by molecular design, the polymers with isosorbide and isomanide chiral molecules have been synthesized. The SHG efficiency of these systems was measured with respect to MNA. It has been seen that, as predicted from the theoretical calculation, polyester with the isomanide system showed 175% more SHG efficiency (3.83 times that of MNA) than that of the polymers with the isosorbide system (2.8 times than that of MNA). The theoretical reason was discussed in section **4.3.2.1.c.** From a stereochemical point of

Figure 4.20.
AM1 Optimized Structure of 3 repeating units of **Pol-VI.**

view, it can be explained on the basis of the polar ordering and absence of dipolar interaction. Even though the chiral molecule, isosorbide and the polymer with isosorbide have more ground state dipole moment than the isomanide and isomanide polymer, the more ordered and symmetrically packed bipolar ones are in the latter compared to the former. This is by virtue of the dipole orientation in isosorbide and isomanide. In isomanide, both the -OH groups are oriented in the same direction, while in isosorbide, -OH groups are oriented in the opposite direction. Higher Tg value of isomanide system, confirmed this observation. SHG efficiency is directly proportional to polar ordering of the system. Thus isomanide system has more SHG efficiency than isosorbide system even though its microscopic chiral tensor (β_{xyz} =103.5382) contribution to macroscopic chiral tensor χ_{xyz} is smaller than isosorbide system (β_{xyz} = 128.0857). It can be concluded that the stereochemistry of chiral molecules, through the polar ordering of polymers, plays an important role in achieving highly active polymers capable of second harmonic generation.

4.6. Correlation of theoretical and experimental results

The SHG efficiency has shown similar trends in theoretical calculation and experimental measurements (**Table 4.19**). Polymers with chiral units showed more nonlinear optical susceptibility than MNA in both theory and experiment. Polymer which contains isomanide as the chiral molecule showed maximum second order response in both theoretical calculation and experimental measurements. Polymer which contains isosorbide showed minimum value of β.

Table 4.19: Comparison of theoretical calculation with experimental measurements

Polymer	β *(10^{-30})esu (Static)*	β *(10^{-30})esu (Dynamic)*	*SHG Efficiency**
Pol-II	10.23	338.99	2.86
Pol-III	7.86	630.23	2.80
Pol-IV	10.22	708.58	3.83
Pol-VI	10.17	364.99	3.07
Pol-VIII	12.64	478.54	2.99
Pol-0	7.60	4.27	0.95
MNA	4.08	202.40	1.00

*Experimental β values of polymers compared with that of MNA

Both *ab initio*- CPHF (*Static*) and ZINDO-SOS(*Dynamic*) calculations are in good agreement with the experimental results. Still, the experimental results match more closely with the ZINDO-SOS calculation. As explained earlier, this variation in *static* calculation is because of the derivative formalism rather than the SOS one. In experimental measurements, electrons will go to possible higher energy states; thus higher energy contribution may not be too small to neglect. But *ab initio*-CPHF is numerically more accurate and precise in predicting the trends.

4.7. Conclusion

The influence of chirality can be used to advantage in designing second order nonlinear optical materials. Chiral molecules have no reflection symmetry and occur in two forms that are mirror images of each other. Such molecules are non-centrosymmetric with a nonvanishing electric-dipole allowed second-order response. Theoretical designing of NLO active polymer with high SHG response is in good agreement with the experimental results. Chirality of the polymer systems enhances the nonlinear optical response in two ways: first by increasing the polar order of the polymeric system and second by chiral contributions. In the systems described here, the chirality of Λ helical structure can supplement the directional order of donor-acceptor π

electron system and the dipole units are tilted in one direction along the polymer axis which leads to large values of χ_{zzz}, χ_{xxz}, χ_{zxx}, thus a high second harmonic generation efficiency. At the same time, the over all macroscopic chirality and the presence of chiral monomers in the polyesters increase the value of chiral tensor χ_{xyz}. Since the polar ordering is vital in the case of polymers incorporating polar chiral monomers, the stereochemistry of the chiral monomer plays an important role in designing efficient polymeric SHG materials. The contribution from the chiral component β_{xyz} is also important in designing SHG material, since it determines the macroscopic chiral susceptibility tensor χ_{xyz}, which is one of the four major non vanishing susceptibility tensors of a C_α symmetry group such as Λ helix. An easy and facile way to synthesize thermally stable and crystalline polymeric materials for nonlinear optics are studied which have given good SHG response compared to MNA.

References:

(1) Prasad, P. N.; Williams, D. J. *Introduction to Nonlinear Optical Effects in Molecules and Polymers*; Wiley: New York, **1991**.

(2) Nalwa, H. S.; Miyata S. *Nonlinear Optics of Organic Molecules and Polymers*; CRC Press: New York, **1997**.

(3) Boyd, R. W. *Nonliner Optics;* Academic Press: San Dieago, **1992**.

(4) Giordmaine, J.A. *Phys.Rev.* **1965,** *138*, A 1599.

(5) Rentzepis, P.M.; Giordmaine, J. A.; Wecht, K.W. *Phys. Rev. Lett.* **1976**, *37*, 431.

(6) Verbiest, T.; Clays, K.; Samyn, C.; Wolff, J.; Reinhoudt, D.; Persoons, A. *J Am Chem Soc* **1994**, *116*, 9320.

(7) Verbiest, T.; Elshocht, S. V.; Kauranen, M.; Hellemans, L.; Snauwaert, J.; Nuckolls, C.; Katz, T. J.; Persoons, A. *Science*,**1998** *282*, 913.

(8) Koeckelberghs, G; Vangheluwe, M; Picard, I; De Groof, L; Verbiest, T; Persoons, A; Samyn, C. *Macromolecules* **2004**, *37*, 8530.

(9) Han, S. H.; Belkin, M.A.; Shen, Y. R.; *Phys Rev. B* **2002,** *66*, 165415.

(10) Simpson, G. J; Perry, J. M; Ashmore-Good C. L *Phy. Rev.B* **2002**, *66*, 165437.

(11) Verbiest, T.; Van Elshocht, S.; Persoons, A.; Nuckolls, C.; Phillips, K. E.; Katz,

T. J. *Langmuir* **2001,** *17,* 4685.

(12) Makki, J. J.; Kauranen, M.; Persoons, A.; *Phy. Rev. B.* **1995,** *51,* 1425.

(13) Walba, D.M.; Xiao, L.; Keller, P.; Shao, R.F.; Link, D.; Clark, N.A. *Pure and Appl. Chem.* **1999,** *71* 2117.

(14) Bahulayan, D.; Thomas, V.; Sreekumar, K. *Proc SPIE, Smart Mater, Struct. MEMS* **1998,** *3321,* 413.

(15) Maniram, K. A.; Sreekumar, K. *Proc SPIE, Smart Mater, Struct. MEMS* **1998,** *3321,* 67.

(16) Bahulayan, D.; Sreekumar, K. *J. Mater. Chem.* **1999,** *9,* 1425.

(17) Burland, D. M.; Miller, R. D.; Walsh, C. A. *Chem. Rev.* **1994,** *94,* 31.

(18) Angiolini, L.; Caretti, D.; Giorgini, E. S. *Polymer* **2001,** *42,* 4005.

(19) Sandhya, K. Y. Pillai, C.K.S.; Tsutsumi, N. *Prog Polym. Sci.* **2004,** *29,* 45.

(20) Bouman, M. M.; Haviga, E. E.; Hanseen, R. A. J.; Meijer, E. W. *Mol. Cryst. Liq. Cryst.* **1994,** *256,* 439

(21) Hohenberg, P.; Kohn, W. *Phys. Rev.* **1964,** *136,* B864.

(22) Kohn, W.; Sham, L. J. *Phys. Rev.* **1965,** *140,* A1133.

(23) Salahub, D. R.; Zerner, M. C. *The Challenge of d and f Electrons;* ACS: Washington, D.C., **1989.**

(24) Parr R. G.; Yang, W. *Density-Functional Theory of Atoms and Molecules;* Oxford Univ. Press: Oxford, **1989.**

(25) Ridley, J.; Zerner, M. C. *Theor. Chim. Acta* **1973,** *32,* 111.; Bacon, D.; Zerner, M. C. *Theor. Chim. Acta* **1979,** *53,* 21

(26) Gerratt, J.; Mills, I. M.; *J. Chem. Phys.* **1968** *49,* 1719

(27) Karna S. P.; Dupuis, M. *J. Comp. Chem.* **1991,** *12,* 487

(28) Karna S. P.; Dupuis, M. *J Chem. Phys. Lett.* **2000,** *319,* 595

(29) Dewar, M. J. S.; Zoebisch, E. G.; Healy, E. F.; Stewart, J. J. P *J. Am. Chem. Soc.* **1985,** *107,* 3902

(30) Kanis, D. R.; Ratner, M. A.; Marks, T .J. *Chem. Rev.* **1994,** 94,195.

(31) Lalama, S. J.; Garito, A. F. *Phys. Rev. A* **1979,** *20,* 20

(32) Ouder, J. L.; and Chemla, D. S. *J. Chem. Phys.* **1977,** *66,* 2664

(33) Ouder, J. L *J. Chem. Phys.* **1977**, *67*, 446

(34) Ouder, J. L.; Zyss, J. *Phys. Rev. A* **1982**, *26*, 2016

(35) Simpson, G. J. *Chem.Phys. Chem.* **2004**, *5*, 1301

(36) Bishop, D. M. *Adv. Chem. Phys.* **1998**, 104,1

(37) Simpson, G. J. *J. Chem. Phys.* **2002**, *117*, 3398

(38) Simpson, G. J.; Perry J. M.; Ashmore-Good, C. L. *Phys. Rev. B.* **2002**, *66*, 165437

(39) Tsunekawa, T.; Yamaguchi, K. *Chem. Phys. Lett.* **1992**,*190*,533

(40) Tsunekawa, T.; Yamaguchi, K. *J. Phys. Chem.* **1992**,*96*, 10268

(41) Organic synthesis, Vol 79, 125

(42) Fieser, L. F; Fieser, M. *Reagents for organic synthesis*; John Wiely and Sons: New York, **1982**

(43) Schwartz, *Chem.Eng. News* **1978**, *24*, 88

(44) Perrin D. D.; Armarego, W. L. F. *Purification of Laboratory Chemicals*; Pergamon press: New York, 1980

(45) Heldmann, C.; Warner, M. *Macromolecules* **1998**, *31*, 3519.

(46) Zhao, Z. Li,Y.; Zhou, J.; Shena, Y. *Eur. Polym.J.* **2000**, *36*, 2417

(47) Beltrania, T.; Boschb, M.B.; Centorea, R.; Concilio, S.C. *Polymer* **2001**, 42, 4025

(48) Zhang, Y.; Wang, T.; Wada,T.;Sasabe, H. *Polym. J.* **1997**, *29*, 685.

(49) Tedder, J. M.; Venkataraman, K. *The Chemistry of Synthetic Dyes*, Academic Press: New York, 1970

(50) Kumar, S; Neckers, D.C *Chem. Rev.* **1989**, *89*, 17

(51) Joshua, C.P.; Ramadas, P. K. *Synthesis* **1974** 573

(52) M.L. Tomlinson, *J. Chem. Soc.* **1946**, 756

(53) Brydson, J. A. *Plastics Materials*; Iliffe Books: London, **1966**

(54) Kurtz, S. K.; Perry, T. T. *J. Appl. Phys.* **1968**, *39*, 3798